DALTON
FULL PAPER

A combinatorial-like probe on the reactivity of the $\{Pt_2S_2\}$ core of $Pt_2(PPh_3)_4(\mu\text{-}S)_2$ by electrospray mass spectrometry. Synthesis and structures of novel heterometallic sulfide aggregates of gold(III), mercury(II), and tin(IV) with platinum(II)

S.-W. Audi Fong,[a] Woon Teck Yap,[a] Jagadese J. Vittal,[a] T. S. Andy Hor,*[a] William Henderson,*[b] Allen G. Oliver[c] and Clifton E. F. Rickard[c]

[a] *Department of Chemistry, Faculty of Science, National University of Singapore, 3 Science Drive 3, 117543 Singapore. E-mail: chmandyh@nus.edu.sg*
[b] *Department of Chemistry, University of Waikato, Private Bag 3105, Hamilton, New Zealand. E-mail: w.henderson@waikato.ac.nz*
[c] *Department of Chemistry, University of Auckland, Private Bag 92019, Auckland, New Zealand*

Received 23rd January 2001, Accepted 9th May 2001
First published as an Advance Article on the web 18th June 2001

Electrospray mass spectrometry (ESMS) provides a rapid and convenient technique for probing the nucleophilicity of the $\{Pt_2S_2\}$ "butterfly" core. Positive-ion electrospray mass spectra have been recorded for a wide array of aggregates incorporating various metallo-fragments into the $Pt_2(PPh_3)_4(\mu\text{-}S)_2$ **1** moiety. Such combinatorial-like screening allowed a large number of different metal–sulfur interactions to be studied and the resultant heterometallic aggregates postulated. Such postulations were subsequently confirmed by synthetic studies and single-crystal X-ray crystallographic analyses. This approach helped to minimize the "wastage" by focusing on the synthesis of aggregates that were supported by the ESMS evidence. It has resulted in the isolation of a series of novel aggregates such as $\{Au^{III}Pt_2S_2\}$, $\{Hg^{II}Pt_2S_2\}$, and $\{Sn^{IV}Pt_2S_2\}$ in good lab-scale yields. It also led to the trapping and characterization of the monoprotonated product of **1**, which has eluded isolation.

Introduction

The chemistry of heteropolynuclear complexes containing diverse metal fragments is a topic of intense interest[1] especially relevant to the chemistry of some industrially important catalytic processes. Complexes with bridging sulfido ligands have received widespread attention because of their broad applications, from biological systems,[2] applied catalysis,[2a,3] to the chemistry of novel molecular systems.[4] Other main areas of application are the design of homo- and hetero-polynuclear clusters,[5] the self-assembly of supramolecular structures, and the photophysical properties of new luminescent and mesogenic phases.

Our fascination for the extensive chemistry exhibited by the $\{Pt_2S_2\}$ "butterfly" core, in particular $Pt_2(PPh_3)_4(\mu\text{-}S)_2$ **1**, has led us recently to review[6] its usefulness as a neutral metalloligand precursor to higher nuclearity aggregates and clusters. This same enthusiasm is shared by González-Duarte and co-workers who have recently reported some interesting features of the analogous $Pt_2(dppe)_2(\mu\text{-}S)_2$ system.[7] Retrospection reveals two outstanding features of the $\{Pt_2S_2\}$ core: (a) the flexible hinge angle (θ) of the central $\{Pt_2S_2\}$ ring, and (b) the highly pronounced nucleophilicity of the lone pairs on the two μ-sulfido ligands. Together, these features adapt the $\{Pt_2S_2\}$ core to the requirements of a variety of ML_mX_n (M = heterometal; L = ligand; X = halide or pseudohalide) compounds, displacing X^- and affording aggregates of the type $[(Ph_3P)_4Pt_2(\mu_3\text{-}S)_2\text{-}ML_m]^{n+}(X^-)_n$. Based on this knowledge, we have prepared a variety of homo- and hetero-metallic aggregates based on the $\{Pt_2S_2\}$ core. The resultant aggregates support a variety of coordination geometries at the heterometal; *viz.* linear,[8] angular,[9] T-shaped,[10] Y-shaped,[11] tetrahedral,[12] square planar,[13] square pyramidal,[12,13b] and distorted trigonal prismatic.[14] This synthetic approach has been extended to heteropolymetallic clusters.[15] Although one would expect that a similar chemistry could be envisaged for the palladium(II), selenide and other analogues, reports on such aggregates remain limited.[16] In view of the utility and versatility of **1** and other compounds as metalloligands, it would be ideal if there exists a routine method that provides a rapid, accurate, sensitive, and definitive identification of the reaction products that are formed when **1** reacts with potential electrophiles or Lewis acids. Such a methodology, which is combinatorial-like, would also greatly accelerate the synthetic plans for new heterometallic aggregates and clusters. Complex **1** is used as a model study in this work. In principle, the method can be applied to any other metalloligands that are Lewis basic.

The development of electrospray mass spectrometry (ESMS) by Yamashita and Fenn[17] has provided a powerful technique for analyzing multiply charged ions, primarily applied to large biomolecules[18] such as proteins and oligonucleotides[19] and later to various charged inorganic[20] and organometallic[21] species in solution. Recently, ESMS was also applied in the characterization of thiometal complexes and thiolate-capped chalcogenide cadmium clusters.[22] In contrast to conventional MS methods, which spawn a lot of undesirable fragment ions in the mass spectra, the ESMS technique usually gives simpler spectra. It affords rapid determination of molecular mass accurately with high sensitivity. It is thus ideally suited to the study of polar, high molecular weight molecules. This unique ability presented an ideal opportunity for us to: (a) probe the reactivity of **1** with an array of main group and transition metal compounds; (b) identify conclusively any new species formed *in situ*, based on comparison of the molecular ion isotope distribution patterns with the theoretical patterns calculated using the Isotope computer program;[23] and (c) repeat promising

 DOI: 10.1039/b100789k

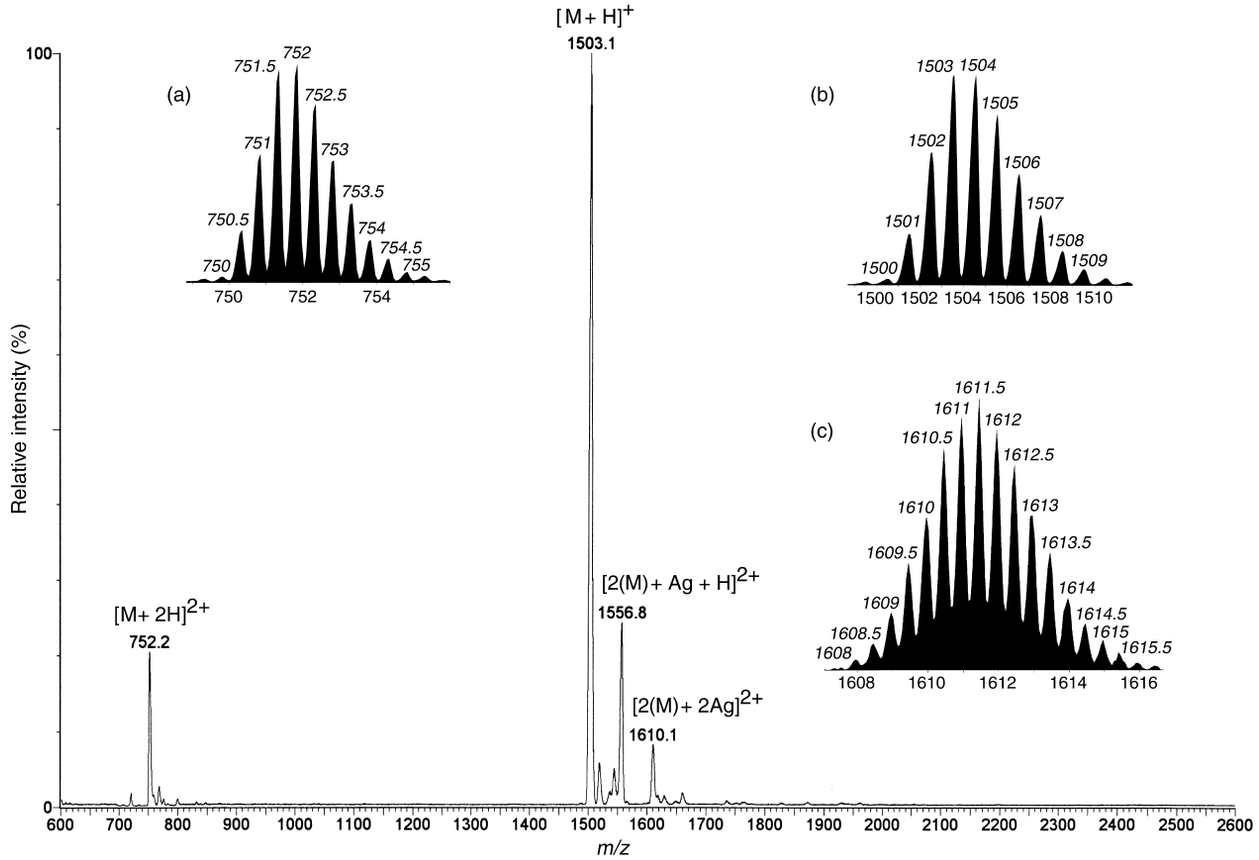

Fig. 1 Positive ion electrospray mass spectrum of a typical solution of $Pt_2(PPh_3)_4(\mu\text{-}S)_2$ **1** in MeOH recorded at a cone voltage of 20 V. The insets show the observed isotope distribution patterns for the ions: (a) $[\mathbf{1} + 2H]^{2+}$, (b) $[\mathbf{1} + H]^{+}$ **2**, and (c) $[2(\mathbf{1}) + 2Ag]^{2+}$.

"ESMS reactions" on a laboratory scale. The formation of cationic complexes from **1** and Lewis acids is ideally suited to this form of ESMS probe. This simple three-step approach has provided much insight into the reactivity of **1** and has resulted in our syntheses of many hitherto unknown heterometallic aggregates reported herein. Such a systematic look at the reactivity of **1** was previously hindered by its low solubility in a wide variety of solvents. The requirement by the ESMS technique of only very dilute solutions for analysis is especially advantageous for the analysis of compounds where other techniques requiring greater solubility, *e.g.* NMR, is not possible.

We have successfully adapted the inherent "softness" of the ESMS ionization technique to provide a preliminary "screening" of the reactivity of a reactant with a large variety of transition metal complexes to ascertain if a particular reaction is indeed feasible prior to a lab-scale synthesis. In this report, we have observed a surprisingly good correlation between the ES mass spectra obtained and synthesis-scale reactions. Through this simple but potentially powerful methodology, we have successfully synthesized and characterized many new aggregates of **1**, such as those containing organo-gold(III), -mercury(II), and -tin(IV) reported here. In addition, as previously reported for other systems,[24] the ES mass spectra also provide useful insight into the mechanisms of formation as well as the fragmentation processes involved in some of these complexes. We are also able to demonstrate that transition metal complexes that have a *cis* arrangement of halides are more likely to react with **1** to form new heterometallic aggregates.

Results and discussion

(1) ES mass spectra of $Pt_2(PPh_3)_4(\mu\text{-}S)_2$ 1 with various compounds

(a) Some general observations on the parent complex 1. ES mass spectra of pure samples of complex $Pt_2(PPh_3)_4(\mu\text{-}S)_2$ **1** have been obtained under various conditions, revealing its propensity to pick up different adventitious positive ions in solution. The ES mass spectrum of a typical suspension of **1** in MeOH is shown in Fig. 1. The mass spectrum consists of peaks due to $[\mathbf{1} + 2H]^{2+}$ (*m*/*z* 752), $[\mathbf{1} + H]^{+}$ (*m*/*z* 1504), $[2(\mathbf{1}) + Ag + H]^{2+}$ (*m*/*z* 1557), and $[2(\mathbf{1}) + 2Ag]^{2+}$ (*m*/*z* 1611). This is not surprising since the high nucleophilicity of the two μ-sulfide centers would result in **1** picking up protons or alikes from the protic solvent or media. This observation was confirmed when addition of a drop of dilute formic acid to this mixture resulted in a sharp increase in the intensity of the peak at *m*/*z* 752. Interestingly, when a drop of dilute HCl was added, a new peak attributed to $[\mathbf{1} + 2H + Cl]^{+}$ (*m*/*z* 1538) was observed. In addition, there is also a strong tendency for complex **1** to pick up adventitious Ag^{+} ions, small quantities of which may persist within the mass spectrometer system from earlier runs; species like $[2(\mathbf{1}) + Ag + H]^{2+}$ (*m*/*z* 1557) and $[2(\mathbf{1}) + 2Ag]^{2+}$ (*m*/*z* 1611) are observed. The latter has been isolated and crystallographically reported.[10] These species, along with those of the protonated species, are manifested in mixtures where **1** does not exhibit any reaction with the transition metal complex present. As such, the presence of these peaks in a given run can be interpreted as a non-reaction. Such mixtures often give a suspension in MeOH due to the insolubility of **1**. A clear and transparent solution strongly indicates the formation of an ionic product between **1** and the complex under investigation. A table summarizing the relative intensities and *m*/*z* values in each case is given (Table 1), along with a schematic representation (Scheme 1). From the insights gained through this ESMS study, we have successfully synthesized the $[(\mathbf{1}) + H]^{+}$ species in the lab and recently reported the novel complex $[Pt_2(PPh_3)_4(\mu\text{-}S)(\mu\text{-}SH)][PF_6]$ **2**.[25] This complex is related to the monomethylated complex reported earlier.[26] Its existence has been proposed but its isolation has not been achieved prior to this report, primarily due to its easy decomposition, presumably after further alkylation or protonation.

Table 1 Cationic species observed in the ES mass spectra for $Pt_2(PPh_3)_4(\mu\text{-}S)_2$ **1** with various adventitious ions present; solvent MeOH, cone voltage 20 V

Mixture	Principal ions (*m*/*z*, %)
1	$[\mathbf{1} + 2H]^{2+}$ (752, 22), $[\mathbf{1} + H]^{+}$ (1504, 100), $[2(\mathbf{1}) + Ag + H]^{2+}$ (1557, 25), $[2(\mathbf{1}) + 2Ag]^{2+}$ (1611, 8)
1 + HCO_2H	$[\mathbf{1} + 2H]^{2+}$ (752, 73), $[\mathbf{1} + H]^{+}$ (1504, 100)
1 + HCl	$[\mathbf{1} + 2H]^{2+}$ (752, 22), $[\mathbf{1} + H]^{+}$ (1504, 47), $[\mathbf{1} + 2H + Cl]^{+}$ (1538, 100)
1 + $AgNO_3$	$[2(\mathbf{1}) + Ag + H]^{2+}$ (1557, 33), $[2(\mathbf{1}) + 2Ag]^{2+}$ (1611, 100)

Table 2 Cationic species observed in the ES mass spectra for **1** with various 2,4-pentanedionato-*O*,*O*′ (acac) complexes; cone voltage 20 V

Mixture	Solvent	Principal ions (*m*/*z*, %)
1 + $Al(acac)_3$	MeOH	$[\mathbf{1} + 2H]^{2+}$ (752, 27), $[\mathbf{1} + H]^{+}$ (1504, 100), $[\mathbf{1} + 2H + Cl]^{+}$ (1538, 15)
1 + $VO(acac)_2$	MeOH	$[Pt(PPh_3)_2(acac)]^{+}$ (818, 28), $[(\mathbf{1})VO(OMe)_2]^{+}$ (1632, 100)
	EtOH	$[(\mathbf{1})VO(OEt)_2]^{+}$ (1660, 100)
1 + $Cr(acac)_3$	MeOH	$[\mathbf{1} + 2H]^{2+}$ (752, 100), $[\mathbf{1} + H]^{+}$ (1504, 8), $[\mathbf{1} + 2H + Cl]^{+}$ (1538, 33)
1 + $Mn(acac)_3$	MeOH	$[Pt(PPh_3)_2(acac)]^{+}$ (818, 100), unidentified (1144, 48)
1 + $Fe(acac)_3$	MeOH	$[(\mathbf{1})Fe(acac)(OMe)]^{+}$ (1689, 100)
	EtOH	$[(\mathbf{1})Fe(acac)(OMe)]^{+}$ (1689, 55), $[(\mathbf{1})Fe(acac)(OEt)]^{+}$ (1703, 100)
1 + $Co(acac)_3$	MeOH	$[\mathbf{1} + 2H]^{2+}$ (752, 66), $[\mathbf{1} + H]^{+}$ (1504, 12), $[\mathbf{1} + 2H + Cl]^{+}$ (1538, 100)

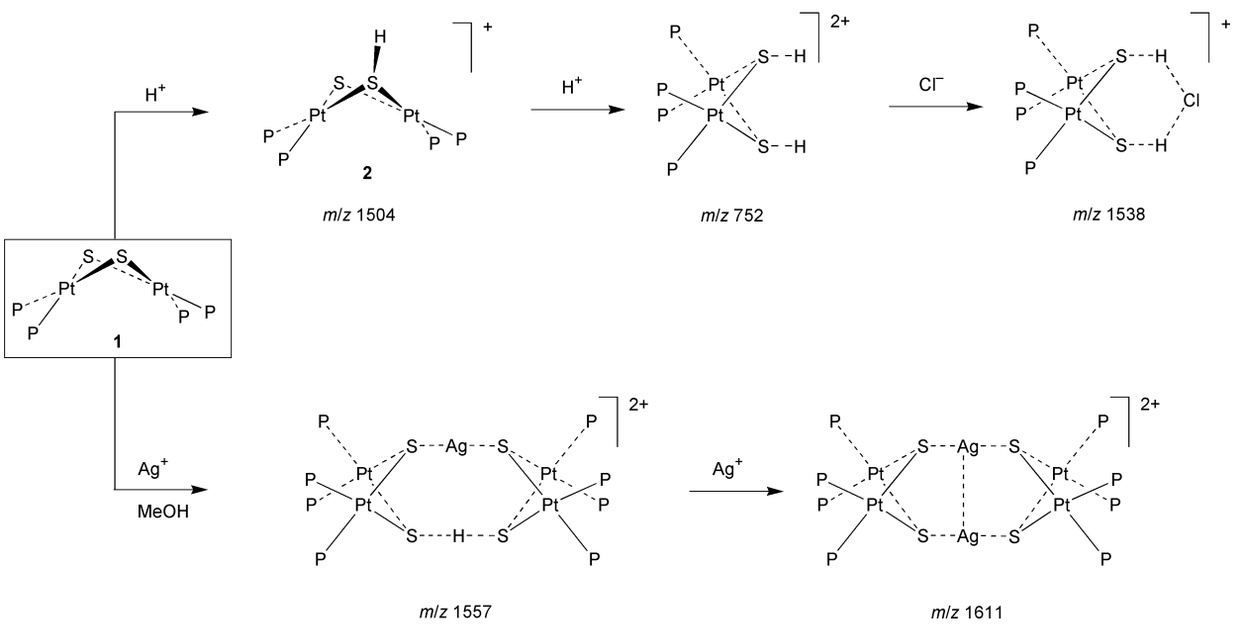

Scheme 1 The reaction of **1** with various adventitious ions present in ESMS; P = PPh_3.

(b) With 2,4-pentanedionato-*O*,*O*′ (acac) complexes. Some interesting observations are seen when complex **1** was treated with various acac complexes. Table 2 provides a summary of some of the species observed under ESMS conditions. With MeOH as solvent and $VO(acac)_2$ as substrate, a major peak was observed at *m*/*z* 1632 which is assigned to the $[(\mathbf{1})VO(OMe)_2]^{+}$ species. The smaller peak at *m*/*z* 818 is assigned to $[Pt(PPh_3)_2(acac)]^{+}$, a species which is manifested due to the breakdown of the $\{Pt_2S_2\}$ ring. The assignment of the major peak is further supported when a peak at *m*/*z* 1660 due to $[(\mathbf{1})VO(OEt)_2]^{+}$ appears with a corresponding change of solvent from MeOH to EtOH. When the substrate was changed to $Fe(acac)_3$ in MeOH a single peak at *m*/*z* 1689 due to $[(\mathbf{1})Fe(acac)(OMe)]^{+}$ was observed. A change of solvent to EtOH gave an additional peak at *m*/*z* 1703 due to $[(\mathbf{1})Fe(acac)(OEt)]^{+}$. The presence of residual MeOH in the capillary system accounts for the smaller peak due to $[(\mathbf{1})Fe(acac)(OMe)]^{+}$ (*m*/*z* 1689) in this case. All other acac complexes gave peaks at *m*/*z* 752, 1504, and 1538, respectively assigned as $[\mathbf{1} + 2H]^{2+}$, $[\mathbf{1} + H]^{+}$, and $[\mathbf{1} + 2H + Cl]^{2+}$. These species were normally observed when reactions did not occur or when **1** was in excess.

(c) With mercury compounds. Given the especially high thiophilicity of mercury, it was interesting to investigate how **1** interacts with various mercury compounds, ranging from mercury halides and mercury–phosphine complexes, to organomercury chlorides. Some earlier Hg^{II}/Pt^{II} work was reported by Mingos and co-workers.[13b] The predominant species detected in this series of ES mass spectra are given in Table 3.

The ES mass spectrum of a mixture of **1** with $HgCl_2$ consists of the expected peaks due to $[(\mathbf{1})(HgCl)_2]^{2+}$ (*m*/*z* 988), $[(\mathbf{1})_2Hg]^{2+}$ (*m*/*z* 1603), and $[(\mathbf{1})HgCl]^{+}$ (*m*/*z* 1739); the proportion of each species varies according to the reaction stoichiometry (see Scheme 2). With $HgCl_2$ as the limiting reagent, further attack of $[(\mathbf{1})HgCl]^{+}$ by any excess of **1** gives the peak due to $[(\mathbf{1})_2Hg]^{2+}$. In an excess of $HgCl_2$, $[(\mathbf{1})_2Hg]^{2+}$ is no longer observed, and the $[(\mathbf{1})(HgCl)_2]^{2+}$ species dominates as each μ-sulfide in **1** takes on an additional {HgCl} fragment. The observation of a peak due to $[(\mathbf{1})_2Hg]^{2+}$ illustrates the ability of mercury(II) to adopt any coordination number from two to four in the presence of sulfur donors. This species was previously reported by Mingos and co-workers as $[(\mathbf{1})_2Hg][BPh_4]_2$.[13b]

All the organomercury chlorides RHgCl under study react with **1** to give the predominant species $[(\mathbf{1})HgR]^{+}$. In the presence of an excess of RHgCl there is a marked shift in equilibria towards $[(\mathbf{1})(HgR)_2]^{2+}$. Fig. 2, for example, shows a mixture of **1** and PhHgCl with peaks corresponding to the species

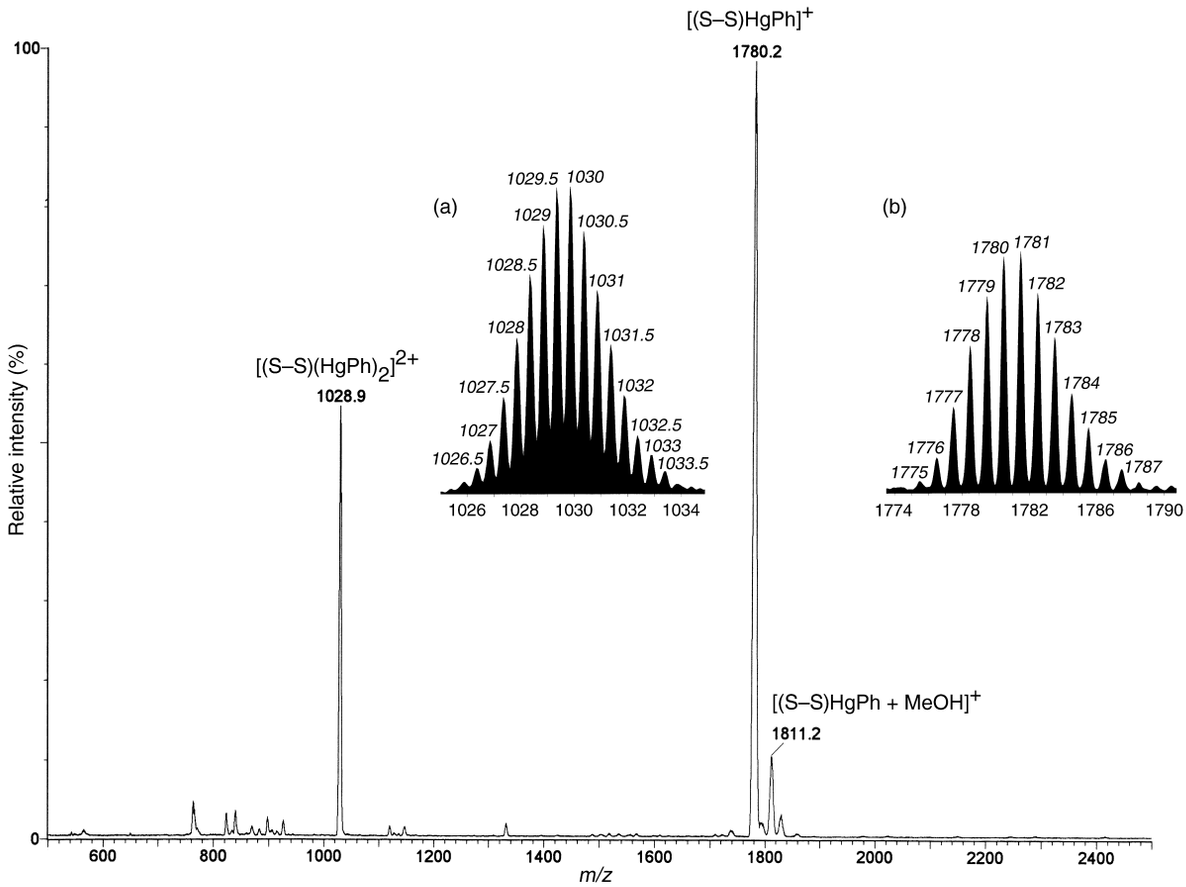

Fig. 2 Positive ion electrospray mass spectrum of an approx. 1 : 1 mixture of **1** with PhHgCl in MeOH recorded at a cone voltage of 20 V. The insets show the observed isotope distribution patterns of the ions (a) $[(\mathbf{1})(HgPh)_2]^{2+}$, and (b) $[(\mathbf{1})HgPh]^{+}$ **3a**.

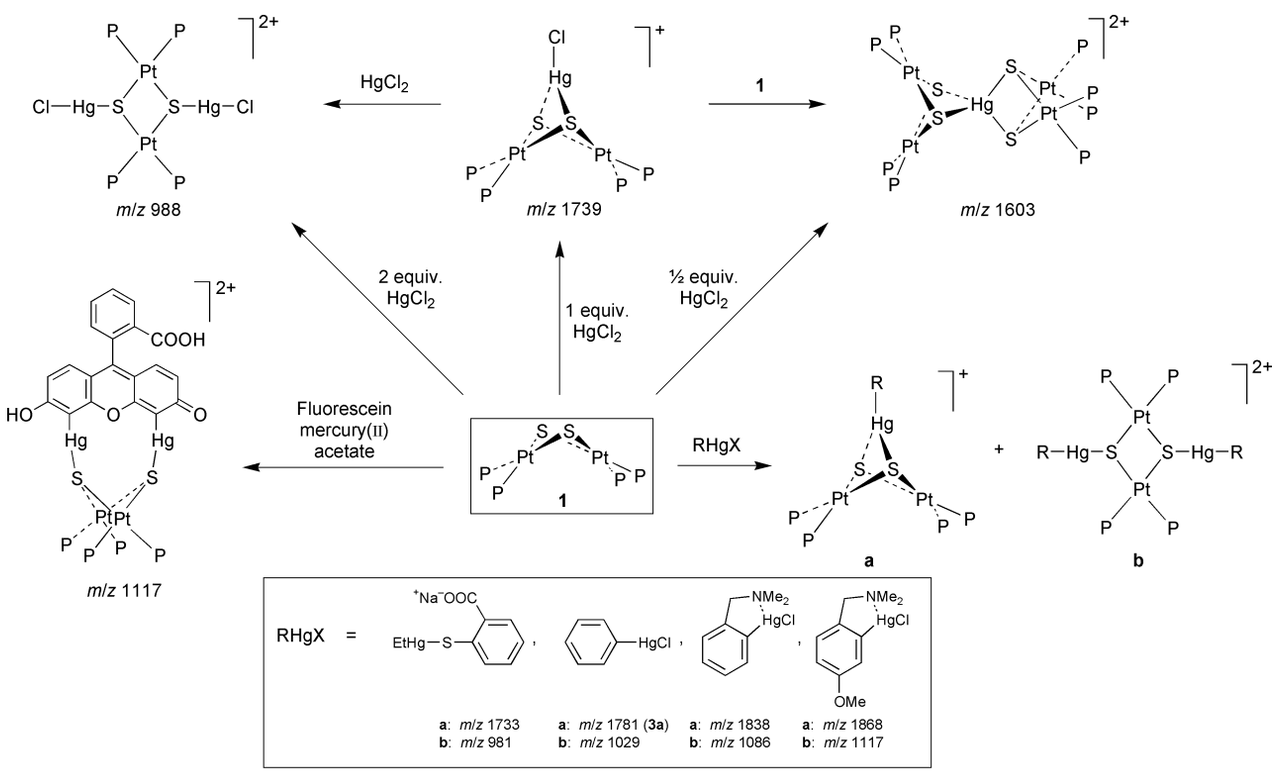

Scheme 2 Observed species for the reaction of **1** with $HgCl_2$ and various organomercury(II) complexes under ESMS conditions; P = PPh_3.

$[(\mathbf{1})(HgPh)_2]^{2+}$ (*m*/*z* 1029, 52%) and $[(\mathbf{1})HgPh]^{+}$ (*m*/*z* 1781, 100%). With an excess of PhHgCl, the relative intensities are reversed; the *m*/*z* 1029 peak increases to 100% while the *m*/*z* 1781 peak drops to 12%. With time, the latter peak diminishes and one should thus expect a lab-scale reaction between excess of PhHgCl and **1** to yield almost exclusively $[(\mathbf{1})(HgPh)_2]^{2+}$ while another with HgPhCl as limiting reagent should favor a greater proportion of $[(\mathbf{1})HgPh]^{+}$. When Thiomersal (EtHg-$SC_6H_4CO_2^{-}Na^{+}$) was used as a source of {EtHg} the analogous ethylmercury derivatives of **1** were observed, *viz.* $[(\mathbf{1})(HgEt)_2]^{2+}$

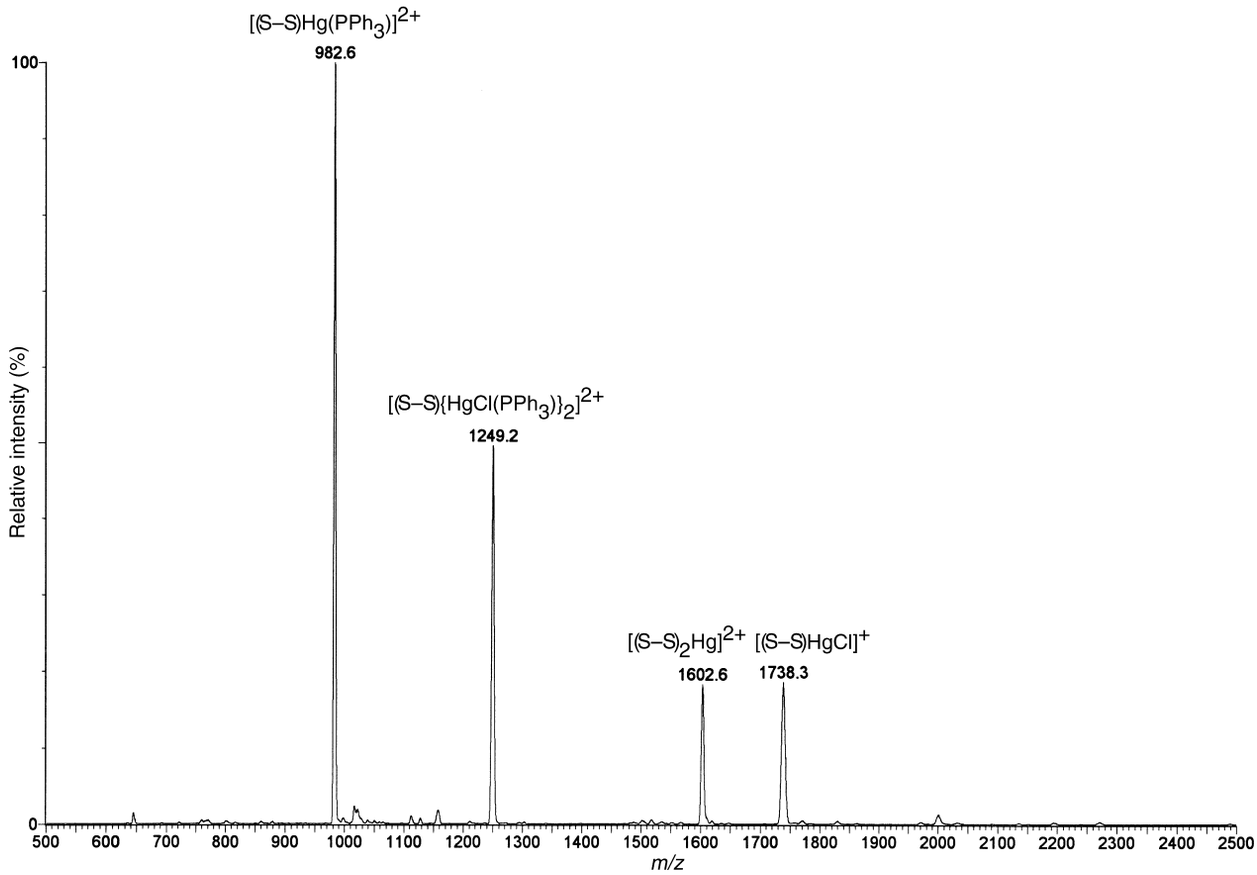

Fig. 3 Positive ion electrospray mass spectrum of a mixture of **1** with $HgCl_2(PPh_3)_2$ in MeOH recorded at a cone voltage of 20 V.

(*m*/*z* 981) and $[(\mathbf{1})HgEt]^+$ (*m*/*z* 1733), along with the same variation of relative intensities according to the amount of {EtHg} added. Another interesting species in the form of $[(\mathbf{1})Hg\text{^}Hg]^{2+}$ (*m*/*z* 1117) was observed when fluoresceinmercury(II) acetate was used [where Hg^Hg represents the fluoresceinmercury(II) moiety]. Many of these reactions have been repeated on synthetic scales and found to be in good agreement with these observations. Similarly, mercurated derivatives of *N*,*N*-dimethylbenzylamine were also found to react with **1**. The ES mass spectrum of a mixture of **1** and $HgCl(\eta^2\text{-}C_6H_4CH_2NMe_2\text{-}C^2,N)$ showed two peaks due to $[(\mathbf{1})\{Hg(\eta^2\text{-}C_6H_4CH_2NMe_2)\}_2]^{2+}$ (*m*/*z* 1086) and $[(\mathbf{1})Hg(\eta^2\text{-}C_6H_4CH_2NMe_2)]^+$ (*m*/*z* 1838). The analogous reaction with $HgCl(\eta^2\text{-}4\text{-}MeOC_6H_3CH_2NMe_2\text{-}C^2,N)$ gave peaks at *m*/*z* 1117 and 1868, due to $[(\mathbf{1})\{Hg(\eta^2\text{-}MeOC_6H_3CH_2NMe_2)\}_2]^{2+}$ and $[(\mathbf{1})Hg(\eta^2\text{-}MeOC_6H_3CH_2NMe_2)]^+$, respectively. In either case, the incoming $\{Pt_2S_2\}$ core was only able to displace chlorides from these complexes. In comparison with the $HgBr_2$(dppe) complex described later, the presence of an interaction between the electron-donating, pendant dimethylamine group and the mercury center derives more robustness from the 5-membered rings thus formed. This is aided by the formal negative charge of the *N*,*N*-dimethylbenzylamine ligands compared to a neutral dppe. Representations of these observed products are also outlined in Scheme 2.

The use of mercury–phosphine complexes gave some interesting observations. The ES mass spectrum of a mixture of **1** and $HgCl_2(PPh_3)_2$ (see Fig. 3) gave four main species: $[(\mathbf{1})Hg(PPh_3)]^{2+}$ (*m*/*z* 983), $[(\mathbf{1})\{HgCl(PPh_3)\}_2]^{2+}$ (*m*/*z* 1250), $[(\mathbf{1})_2Hg]^{2+}$ (*m*/*z* 1603), and $[(\mathbf{1})HgCl]^+$ (*m*/*z* 1739), in order of increasing *m*/*z* values. The presence of these species, other than that of the expected $[(\mathbf{1})\{HgCl(PPh_3)\}_2]^{2+}$, can be interpreted in terms of the lability of PPh_3 and chloride. We have recently done a structural study into these compounds.[27] In comparison, when **1** was mixed with $HgBr_2$(dppe), the ES mass spectrum indicated the presence of the following species: $[(\mathbf{1})Hg(dppe)]^{2+}$ (*m*/*z* 1051), $[(\mathbf{1})_2Hg]^{2+}$ (*m*/*z* 1603), $[(\mathbf{1})HgBr]^+$ (*m*/*z* 1783), and $[(\mathbf{1})HgBr(dppe)]^+$ (*m*/*z* 2182) while an analogous peak due to $[(\mathbf{1})\{HgBr(dppe)\}_2]^{2+}$ was absent. It is noteworthy that $[(\mathbf{1})Hg(\eta^2\text{-}dppe)]^{2+}$ has also been synthesized and characterized crystallographically.[13b] Scheme 3 provides a summary of these observations.

From this ESMS-assisted study it is evident that mercury compounds have an inherently high affinity for the sulfides on the $\{Pt_2S_2\}$ core. In order to accommodate some of the structures observed the mercury atom has to be versatile enough to adopt different coordination modes, ranging from linear, to trigonal planar, to tetrahedral, and even an unusual T shape as structurally determined in $[(Ph_3P)_4Pt_2(\mu_3\text{-}S)_2HgPh]^+$ **3a** and $[(Ph_3P)_4Pt_2(\mu_3\text{-}S)_2Hg(PPh_3)]^{2+}$.[27] This paper will also detail the synthetic, spectroscopic and structural aspects of some organomercury derivatives of **1** that have spawned from insights gained through this ESMS study. These new examples serve to underscore the utility of ESMS in the preliminary detection and characterization of such new compounds.

(d) With gold compounds. To date, the only reported aggregates of **1** with gold(I) are $[(Ph_3P)_4Pt_2(\mu_3\text{-}S)_2Au(PPh_3)]^+$, $[(Ph_3P)_4Pt_2(\mu_3\text{-}S)_2(AuCl)_2]$,[8] and $[(Ph_3P)_4Pt_2(\mu_3\text{-}S)_2Au_2(dppf)]^{2+}$.[28] A summary of the predominant species obtained from **1** with a number of complexes of Au^I and Au^{III} is given in Table 4. This is the first indication that it is possible to assemble Pt^{II}/Au^{III} sulfide aggregates which are unknown in the current literature.

The ES mass spectrum of **1** with $AuCl(PPh_3)$ gives two species: $[(\mathbf{1})\{Au(PPh_3)\}_2]^{2+}$ (*m*/*z* 1211) and $[(\mathbf{1})\{Au(PPh_3)\}]^+$ (*m*/*z* 1962). Analogously, with $AuCl(2\text{-}NC_5H_4PPh_2)$, peaks at *m*/*z* 1212 and 1963, assigned to $[(\mathbf{1})\{Au(2\text{-}NC_5H_4PPh_2)\}_2]^{2+}$ and $[(\mathbf{1})\{Au(2\text{-}NC_5H_4PPh_2)\}]^+$, respectively, are readily observed. The predominant species arising from **1** and $Au_2Cl_2(\mu\text{-}dppf)$ is $[(\mathbf{1})Au_2(\mu\text{-}dppf)]^{2+}$ (*m*/*z* 1226), with a minor peak (5%) at *m*/*z* 2270 due to $[(\mathbf{1})\{Au(\eta^1\text{-}dppfO)\}]^+$.

Table 3 Cationic species observed in the ES mass spectra of **1** with various mercury(II) compounds; solvent MeOH, cone voltage 20 V

Mixture	Principal ions (*m*/*z* %)
Mercury halide complexes	
1 + $HgCl_2$ (1 : 1)	$[(\mathbf{1})(HgCl)_2]^{2+}$ (988, 17), $[(\mathbf{1})_2Hg]^{2+}$ (1603, 7), $[(\mathbf{1})HgCl]^{+}$ (1739, 100)
(2 : 1)	$[(\mathbf{1})(HgCl)_2]^{2+}$ (988, 12), $[(\mathbf{1})_2Hg]^{2+}$ (1603, 100), $[(\mathbf{1})HgCl]^{+}$ (1739, 23)
(1 : 2)	$[(\mathbf{1})(HgCl)_2]^{2+}$ (988, 100), $[(\mathbf{1})HgCl]^{+}$ (1739, 42)
Mercury–phosphine complexes	
1 + $HgCl_2(PPh_3)_2$	$[(\mathbf{1})Hg(PPh_3)]^{2+}$ (983, 100), $[(\mathbf{1})\{HgCl(PPh_3)\}_2]^{2+}$ (1250, 50), $[(\mathbf{1})_2Hg]^{2+}$ (1603, 19), $[(\mathbf{1})HgCl]^{+}$ (1739, 20)
1 + $HgBr_2$(dppe)	$[(\mathbf{1})Hg(dppe)]^{2+}$ (1051, 100), $[(\mathbf{1})_2Hg]^{2+}$ (1603, 82), $[(\mathbf{1})HgBr]^{+}$ (1783, 34), $[(\mathbf{1})HgBr(dppe)]^{+}$ (2182, 5)
Organomercury compounds	
1 + HgPhCl	1 equiv. Hg: $[(\mathbf{1})(HgPh)_2]^{2+}$ (1029, 52), $[(\mathbf{1})HgPh]^{+}$ (1781, 100)
	Excess of Hg: $[(\mathbf{1})(HgPh)_2]^{2+}$ (1029, 100), $[(\mathbf{1})HgPh]^{+}$ (1781, 12)
1 + $EtHgSC_6H_4CO_2Na$ (Thiomersal)	1 equiv. Hg: $[(\mathbf{1})(HgEt)_2]^{2+}$ (981, 48), $[(\mathbf{1})HgEt]^{+}$ (1733, 100)
	Excess of Hg: $[(\mathbf{1})(HgEt)_2]^{2+}$ (981, 100), $[(\mathbf{1})HgEt]^{+}$ (1733, 8)
1 + Fluorescein–$Hg_2(OAc)_2$[a]	$[Pt(PPh_3)(MeCN)\{\eta^2\text{-}C_6H_4PPh_2\text{-}C,P\}]^{+}$ (759, 100), $[Pt(PPh_3)_2\{\eta^2\text{-}C_6H_4PPh_2\text{-}C,P\}]^{+}$ (981, 72), $[(\mathbf{1})Hg\hat{}Hg]^{2+}$ (1117, 53)[b]
1 + $HgCl(\eta^2\text{-}C_6H_4CH_2NMe_2\text{-}C^2,N)$	$[(\mathbf{1})\{Hg(\eta^2\text{-}C_6H_4CH_2NMe_2)\}_2]^{2+}$ (1086, 35), $[(\mathbf{1})Hg(\eta^2\text{-}C_6H_4CH_2NMe_2)]^{+}$ (1838, 100)
1 + $HgCl(\eta^2\text{-}4\text{-}MeOC_6H_3CH_2NMe_2\text{-}C^2,N)$	$[(\mathbf{1})\{Hg(\eta^2\text{-}MeOC_6H_3CH_2NMe_2)\}_2]^{2+}$ (1117, 100), $[(\mathbf{1})Hg(\eta^2\text{-}MeOC_6H_3CH_2NMe_2)]^{+}$ (1868, 83)

[a] No initial reaction; mixture allowed to stand for 10 d. [b] Hg^Hg denotes the fluorescein–Hg_2 species.

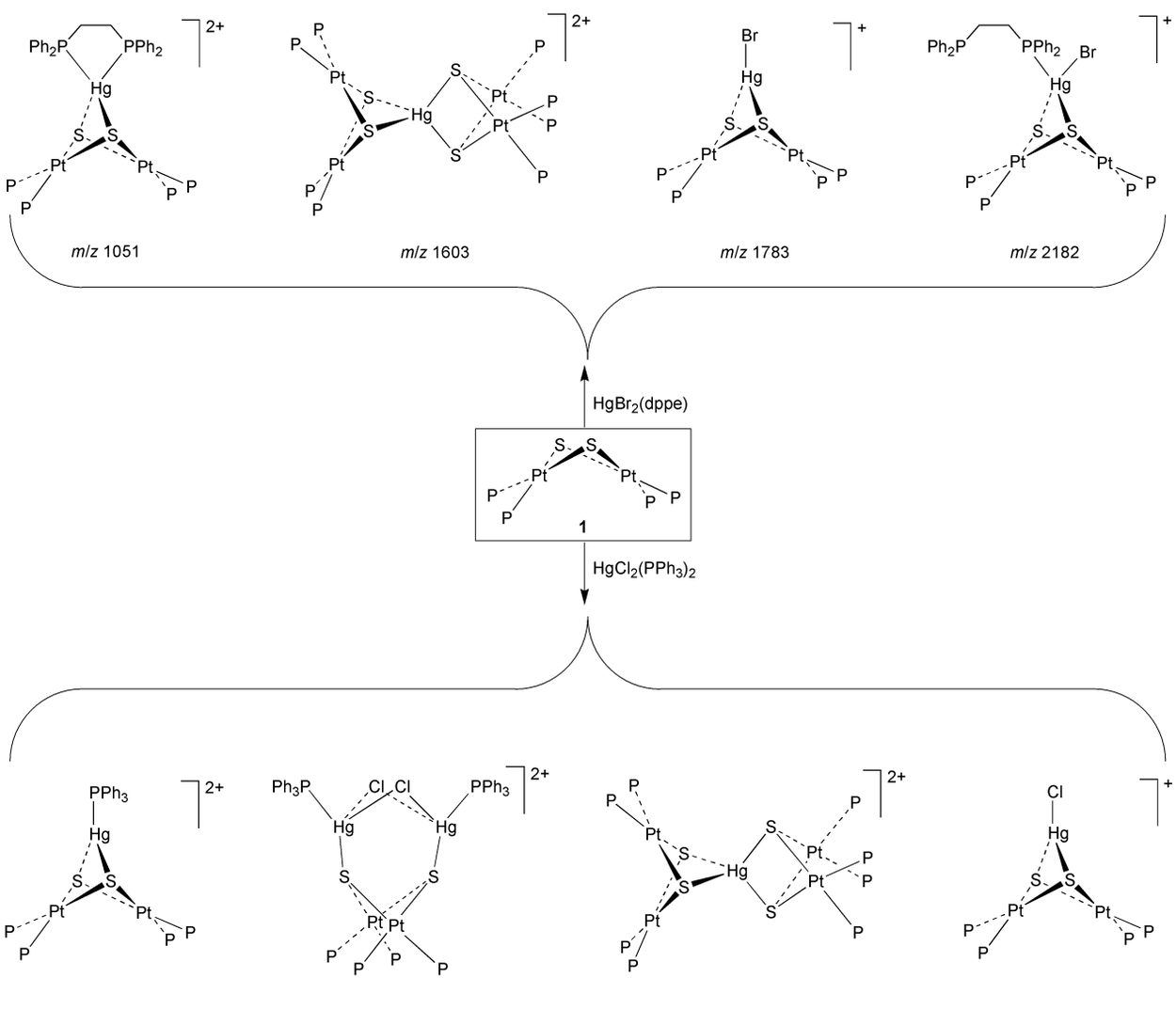

Scheme 3 Major species observed for the reaction of **1** with mercury–phosphine complexes under ESMS conditions; P = PPh_3.

We have also investigated the reactions between **1** and some gold(I) thio- and seleno-ether complexes. For example, when a freshly prepared sample of the tetrahydrothiophene (tht) complex AuCl(tht) was added to **1**, the ES mass spectrum (Fig. 4) revealed dominant peaks corresponding to $[(\mathbf{1})\{Au(tht)\}_2]^{2+}$ (*m*/*z* 1036) and $[(\mathbf{1})(AuCl)\{Au(tht)\}]^{+}$ (*m*/*z* 2020).

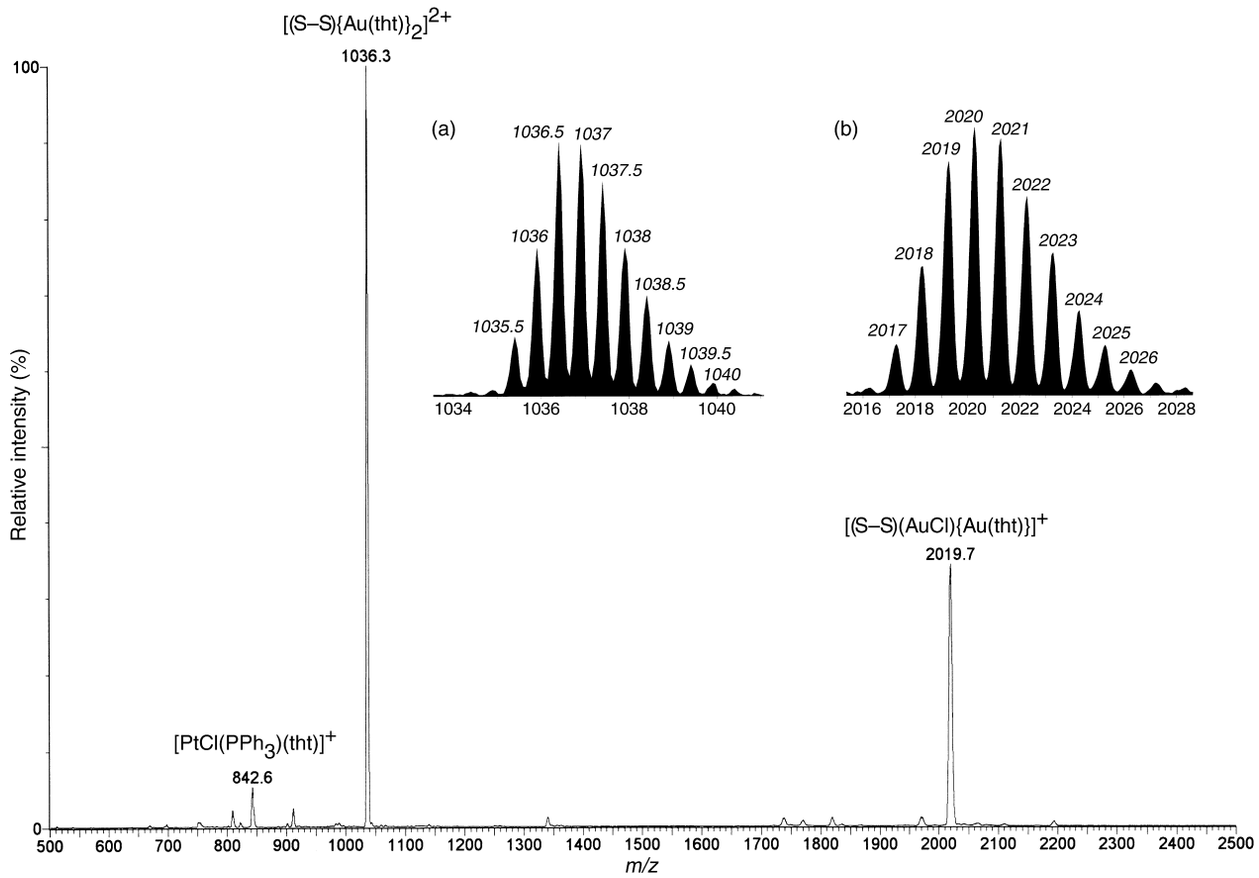

Fig. 4 Positive ion electrospray mass spectrum of an approx. 1 : 1 mixture of **1** with AuCl(tht) in MeOH recorded at a cone voltage of 20 V. The insets show the observed isotope distribution patterns of the ions: (a) $[(\mathbf{1})\{Au(tht)\}_2]^{2+}$, and (b) $[(\mathbf{1})(AuCl)\{Au(tht)\}]^{+}$.

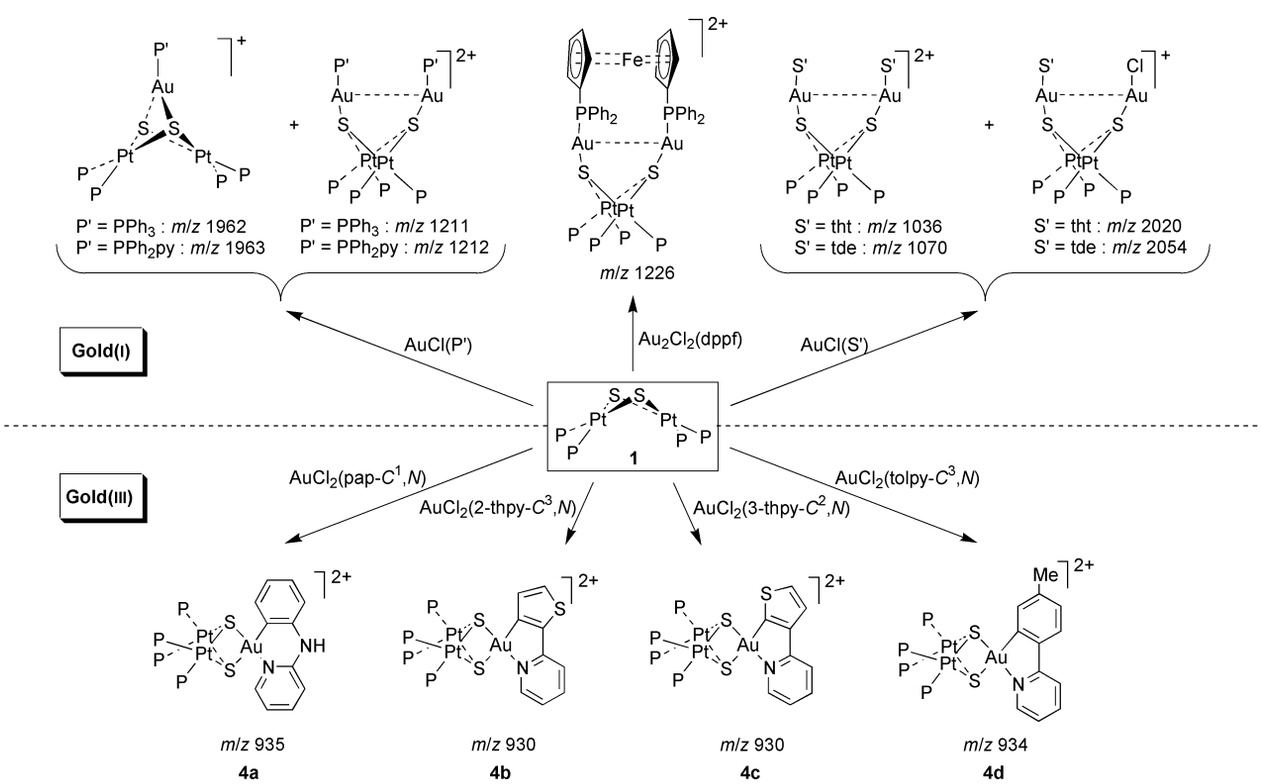

Scheme 4 Observed species for the reaction of **1** with various gold(I) and gold(III) complexes under ESMS conditions; P = PPh_3.

The counterpart of the latter was not observed in $AuCl(PPh_3)$. This is explained by the higher lability of the Au–Cl bond in $AuCl(PPh_3)$. With $AuCl[S(CH_2CH_2OH)_2]$, generated *in situ* by addition of an excess of thiodiethanol (tde) to $HAuCl_4$, peaks due to $[(\mathbf{1})\{AuS(CH_2CH_2OH)_2\}_2]^{2+}$ (*m/z* 1070) and $[(\mathbf{1})(AuCl)\{AuS(CH_2CH_2OH)_2\}]^{+}$ (*m/z* 2054) are observed. Scheme 4 details these observations as well as those involving the subsequent gold(III) complexes. The selenoether complex $AuCl[Se(CH_2Ph)_2]$, also generated *in situ* from $Se(CH_2Ph)_2$ and $HAuCl_4$, gave analogous products, *viz.* $[(\mathbf{1})\{AuSe(CH_2Ph)_2\}_2]^{2+}$

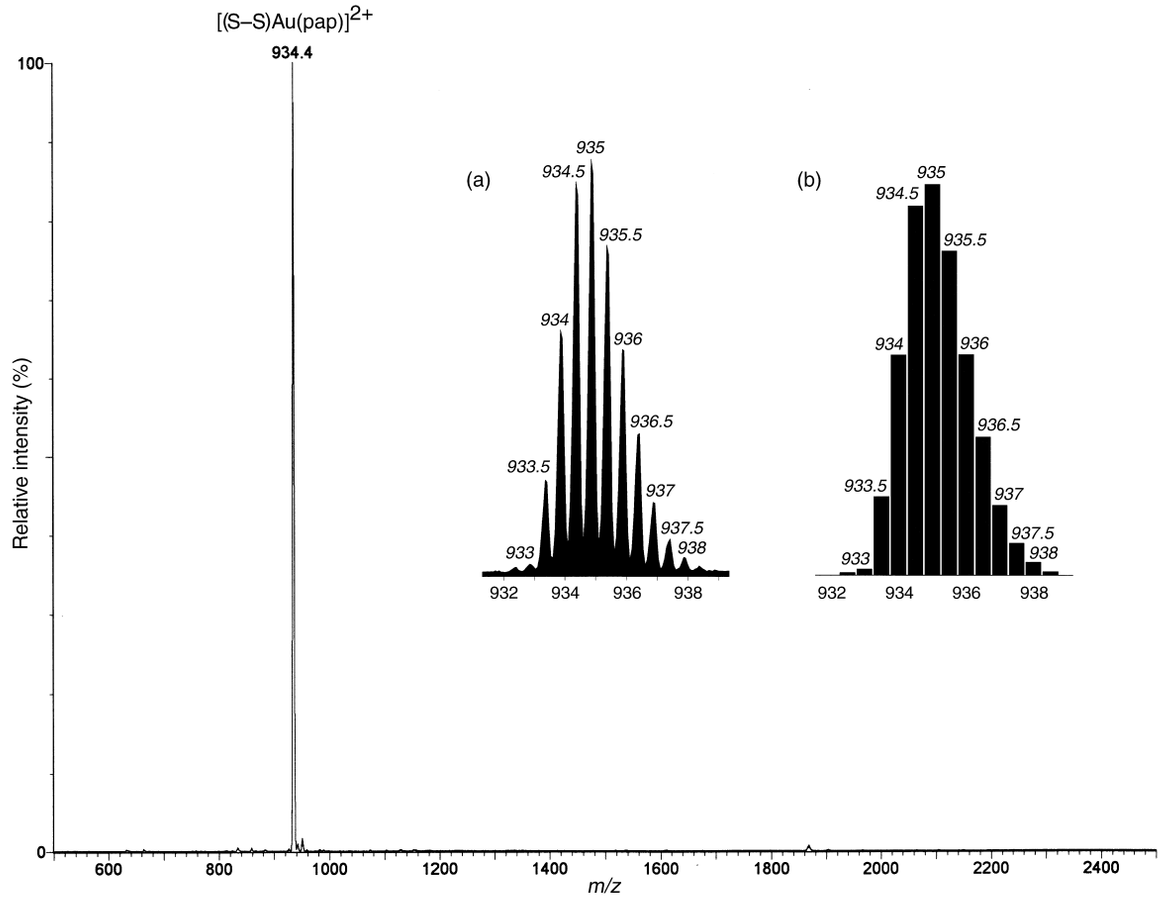

Fig. 5 Positive ion electrospray mass spectrum of an approx. 1 : 1 mixture of **1** with $AuCl_2$(pap-C^1,N) in MeOH recorded at a cone voltage of 20 V. The inset shows the (a) observed and (b) calculated isotope distribution patterns for the principal ion $[(\mathbf{1})Au(pap)]^{2+}$ **4a**.

(*m*/*z* 1214) and $[(\mathbf{1})(AuCl)\{AuSe(CH_2Ph)_2\}]^+$ (*m*/*z* 2194). A peak at *m*/*z* 1771 due to $[(\mathbf{1})AuCl_2]^+$ was probably caused by some unchanged $HAuCl_4$ present.

Although we have recently outlined the isolation and characterization of the apparently facile reaction between **1** and two novel, cycloaurated gold(III) complexes $AuCl_2$(pap-C^1,N) [pap = 2-(2-pyridylamino)phenyl], $AuCl_2$(tolpy-C^3,N) [tolpy = 4-(2-pyridyl)-3-tolyl],[25] we include a discussion here with two new examples: $AuCl_2$(2-thpy-C^3,N) [2-thpy = 2-(2-pyridyl)-3-thienyl], $AuCl_2$(3-thpy-C^2,N) [3-thpy = 3-(2-pyridyl)-2-thienyl]. The tolpy complexes has only recently been synthesized,[29] while the others have been described by Fuchita *et al.*[30]

Fig. 5 shows the ES mass spectrum of **1** with $AuCl_2$-(pap-C^1,N) at a moderate cone voltage of +20 V revealing a single peak (with half-integral isotopic mass patterns) at *m*/*z* 935 due to the intact dication $[(\mathbf{1})Au(pap)]^{2+}$. An investigation into the fragmentation pathway of this new species revealed that it is stable up to a cone voltage of +60 V whereupon dissociation of a PPh_3 occurs, yielding a peak at *m*/*z* 804. Another small peak at *m*/*z* 1867 (8%) is due to loss of the amino proton from the precursor ion. When the cone voltage is raised slightly to +70 V a new peak appears at *m*/*z* 626, assigned as $[Pt(PPh_3)(pap)]^+$, indicating that the $\{Pt_2S_2\}$ core begins to break down under these conditions. The remaining peaks have also increased in intensity at the expense of the precursor dication. At a harsher cone voltage of +80 V cyclometallation of PPh_3 produces $[Pt(PPh_3)_2\{\eta^2\text{-}C_6H_4PPh_2\}]^+$ (*m*/*z* 980) in addition to those species already observed. Both $AuCl_2$(2-thpy-C^3,N) and $AuCl_2$(3-thpy-C^2,N), react with **1** to give isomeric aggregates which differ in the coordination position of the thienyl group. As such, the ESMS spectra of the aggregates each give a strong peak at *m*/*z* 930 corresponding to the isomeric $[(\mathbf{1})Au(2\text{-thpy-}C^3,N)]^{2+}$ and $[(\mathbf{1})Au(3\text{-thpy-}C^2,N)]^{2+}$ species. $AuCl_2$(tolpy-C^3,N) behaves in a similar manner, yielding the intact dicationic analog $[(\mathbf{1})Au(tolpy\text{-}C^3,N)]^{2+}$ (*m*/*z* 934). This precursor species also begins losing its integrity at +60 V, by fragmentation of a PPh_3, to give a peak at *m*/*z* 803. Unlike the 2-(2-pyridylamino)phenyl analog, there is no evidence of a peak due to a loss of H^+. This confirms that the amino proton of the (2-pyridylamino)phenyl can be extruded at high cone voltages. When the pre-cycloaurated complex, $AuCl_3$(tolpy′-N) [tolpy′ = 4-(2-pyridyl)tolyl], was mixed with **1**, an interesting peak at *m*/*z* 1700 assigned to $[(\mathbf{1})_2Au_2]^{2+}$ appeared. This species is analogous to $[(\mathbf{1})_2Ag_2]^{2+}$ which has been reported by Mingos and co-workers[10] and is also observed under ESMS conditions (see Table 1). The facile formation of these new $\{Pt_2S_2Au^{III}\}$ aggregates is facilitated by the increased stability towards reduction (by sulfur-based ligands) of these gold(III) complexes bearing *N*,*C*-cyclometallated ligands.

Reactions of **1** with $HAuCl_4$ and $[Me_4N][AuCl_4]$ lead to breakdown of the $\{Pt_2S_2\}$ core. As a result, fragments such as $[PtCl(PPh_3)_2]^+$ (*m*/*z* 755) readily pick up residual pyridine (py) to give $[PtCl(PPh_3)_2(py)]^+$ (*m*/*z* 834). These species dominate the ES mass spectra while any residual **1** reacts with $[AuCl_4]^-$ to give $[(\mathbf{1})AuCl_2]^+$ (*m*/*z* 1771). These observations suggest that oxidation competes with coordination in determining the fate of the product. Upon coordination $[(\mathbf{1})AuCl_2]^+$ is stable and not oxidizing just as $AuCl_2$(pap-C^1,N) and $AuCl_2$(tolpy-C^3,N) do not oxidize thiols, whereas $[AuCl_4]^-$ and $AuCl_3$(tolpy′-N) do.

(e) With organotin(IV) compounds. Another series that we have studied by this ESMS method are the reactions between **1** and organotin(IV) compounds. While the thallium(I) and lead(II) congeners, *i.e.* $[(Ph_3P)_4Pt_2(\mu_3\text{-}S)_2Tl]^+$ [9b] and $[(Ph_3P)_4Pt_2(\mu_3\text{-}S)_2Pb(NO_3)]^+$,[14] are already known, $\{Pt_2S_2Sn^{IV}\}$ aggregates remain unexplored. This ESMS technique allows us to study the *in situ* reaction of **1** with a series of organotin(IV)

Table 4 Cationic species observed in the ES mass spectra of **1** with various gold compounds; solvent MeOH

Mixture	Cone voltage/V	Principal ions (*m*/*z*, %)
Gold(I) compounds		
1 + $AuCl(PPh_3)$	20	$[(\mathbf{1})\{Au(PPh_3)\}_2]^{2+}$ (1211, 1000), $[(\mathbf{1})Au(PPh_3)]^+$ (1962, 92)
1 + $AuCl(2\text{-}NC_5H_4PPh_2)$	20	$[(\mathbf{1})\{Au(2\text{-}NC_5H_4PPh_2)\}_2]^{2+}$ (1212, 100), $[(\mathbf{1})Au(2\text{-}NC_5H_4PPh_2)]^+$ (1963, 57)
1 + $Au_2Cl_2(\mu\text{-dppf})$	20	$[(\mathbf{1})Au_2(\mu\text{-dppf})]^{2+}$ (1226, 100), $[(\mathbf{1})Au(\eta^1\text{-dppfO})]^+$ (2270, 5)
1 + AuCl(tht)	20	$[PtCl(PPh_3)_2(tht)]^+$ (843, 6), $[(\mathbf{1})\{Au(tht)\}_2]^{2+}$ (1036, 100), $[(\mathbf{1})$ + 2H + $Cl]^+$ (1538, 4), $[(\mathbf{1})(AuCl)\{Au(tht)\}]^+$ (2020, 36)
1 + $AuCl[S(CH_2CH_2OH)_2]$[a]	20	$[(\mathbf{1})\{AuS(CH_2CH_3)_2\}_2]^{2+}$ (1040, 100), $[(\mathbf{1})\{AuS(CH_2CH_2OH)_2\}_2]^{2+}$ (1070, 33), $[(\mathbf{1})(AuCl)\{AuS(CH_2CH_2OH)_2\}]^+$ (2054, 5)
1 + $AuCl[Se(CH_2Ph)_2]$[a]	20	$[PtCl(PPh_3)_2\{Se(CH_2Ph)_2\}]^+$ (1017, 16), $[(\mathbf{1})\{AuSe(CH_2Ph)_2\}_2]^{2+}$ (1214, 14), $[\mathbf{1}$ + 2H + $Cl]^+$ (1538, 17), $[(\mathbf{1})AuCl_2]^+$ (1771, 41), $[(\mathbf{1})(AuCl)\{AuSe(CH_2Ph)_2\}]^+$ (2194, 100)
Gold(III) compounds		
1 + $AuCl_2(pap\text{-}C^1,N)$	20	$[(\mathbf{1})Au(pap)]^{2+}$ (M; 935, 100)
	60	$[M - PPh_3]^{2+}$ (804, 23), $[M]^{2+}$ (935, 100), $[M - H]^+$ (1867, 8)
	70	$[Pt(PPh_3)(pap)]^+$ (626, 12), $[M - PPh_3]^{2+}$ (804, 100), $[M]^{2+}$ (935, 62), $[M - H]^+$ (1867, 10)
	80	$[Pt(PPh_3)(pap)]^+$ (626, 62), $[M - PPh_3]^{2+}$ (804, 100), $[M]^{2+}$ (935, 28), $[Pt(PPh_3)_2\{\eta^2\text{-}C_6H_4\text{-}PPh_2\}]^+$ (980, 31), $[M - H]^+$ (1867, 29)
1 + $AuCl_2(2\text{-thpy-}C^3,N)$	20	$[(\mathbf{1})Au(2\text{-thpy})]^{2+}$ (M; 930, 100)
1 + $AuCl_2(3\text{-thpy-}C^2,N)$	20	$[(\mathbf{1})Au(3\text{-thpy})]^{2+}$ (M; 930, 100)
1 + $AuCl(tolpy\text{-}C^3,N)$	20	$[(\mathbf{1})Au(tolpy)]^{2+}$ (934, 100)
	60	$[M - PPh_3]^{2+}$ (803, 22), $[M]^{2+}$ (934, 100), $[\mathbf{1} + H]^+$ (1504, 3), unidentified (1962, 2)
	80	$[Pt(PPh_3)(tolpy)]^+$ (625, 31), $[M - PPh_3]^{2+}$ (803, 100), $[M]^{2+}$ (934, 17), $[Pt(PPh_3)_2\{\eta^2\text{-}C_6H_4PPh_2\}]^+$ (980, 19), $[\mathbf{1} + H]^+$ (1504, 11), unidentified (1962, 10)
1 + $AuCl_3(tolpy'\text{-}N)$	20	$[\mathbf{1} + 2H]^{2+}$ (752, 28), $[\mathbf{1}$ + 2H + $Cl]^+$ (1538, 55), unidentified (1655, 30), $[(\mathbf{1})_2Au_2]^{2+}$ (1700, 100)
1 + $HAuCl_4$	20	$[PtCl(PPh_3)_2]^+$ (755, 27), $[PtCl(PPh_3)_2(py)]^{2+}$ (834, 100), unidentified (871, 23), $[(\mathbf{1})AuCl_2]^+$ (1771, 43), unidentified (1863, 22)
1 + $[Me_4N][AuCl_4]$	20	$[PtCl(PPh_3)_2]^+$ (755, 45), $[PtCl(PPh_3)_2(py)]^+$ (834, 100), unidentified (892, 65), $[(\mathbf{1})AuCl_2]^+$ (1771, 50)

[a] Generated *in situ* from $HAuCl_4$ and the ligands.

Table 5 Cationic species observed in the ES mass spectra for **1** with various organotin(IV) compounds; cone voltage 20 V

Mixture	Solvent	Principal ions (*m*/*z*, %)
1 + $SnPh_2Cl_2$	MeOH	$[(\mathbf{1})SnPh_2]^{2+}$ (888, 100), $[(\mathbf{1})SnPh_2Cl]^+$ (1812, 32)
1 + $SnMeCl_3$	MeOH	$[(\mathbf{1})SnMeCl]^{2+}$ (836, 88), $[(\mathbf{1})SnMeCl_2]^+$ (1707, 100), $[(\mathbf{1})SnMeCl_2$ + $MeOH]^+$ (1739, 13)
1 + $SnMe_2Cl_2$	MeOH	$[(\mathbf{1})SnMe_2]^{2+}$ (826, 68), $[(\mathbf{1})SnMeCl_2]^+$ (1687, 100), $[(\mathbf{1})SnMeCl_2$ + $MeOH]^+$ (1719, 20)
1 + $SnMe_3Cl$	MeOH	$[(\mathbf{1})SnMe_3]^+$ (1667, 100)
1 + $SnEt_2Cl_2$	MeOH	$[(\mathbf{1})SnEt_2]^{2+}$ (840, 91), $[(\mathbf{1})SnEt_2Cl]^+$ (1715, 100)
1 + $Sn(n\text{-Bu})Cl_3$	MeOH	$[(\mathbf{1})Sn(n\text{-Bu})Cl]^{2+}$ (857, 100), $[(\mathbf{1})Sn(n\text{-Bu})Cl_2]^+$ (1750, 26)
1 + $Sn(n\text{-Bu})_2Cl_2$	MeOH	$[(\mathbf{1})Sn(n\text{-Bu})_2]^{2+}$ (868, 100), $[(\mathbf{1})Sn(n\text{-Bu})_2Cl]^+$ (1771, 68)
1 + $SnPhCl_3$	MeOH	$[(\mathbf{1})SnPhCl]^{2+}$ (867, 100), $[(\mathbf{1})SnPhCl_2]^+$ (1770, 20)
1 + $SnPh_3Cl$	MeCN	$[(\mathbf{1})SnPh_3]^+$ (1853, 100)
1 + $Sn(CH_2Ph)_2Br_2$	MeOH	$[(\mathbf{1})Sn(CH_2Ph)_2]^{2+}$ (902, 100), $[(\mathbf{1})Sn(CH_2Ph)_2Cl]^+$ (1839, 20), $[(\mathbf{1})Sn(CH_2Ph)_2Br]^+$ (1884, 34)

compounds, *viz.* $SnR_nX_{(4-n)}$ (where R = Ph, X = Cl, n = 1–3; R = CH_2Ph, X = Br, n = 2; R = *n*-Bu, X = Cl, n = 1 or 2; R = Et, X = Cl, n = 2; R = Me, n = 1–3). The observed species are summarized in Table 5.

The ESMS spectra of mixtures of complex **1** with the respective $SnR_nX_{(4-n)}$ in MeOH invariably yield analogous products in solution, with the incoming **1** moiety displacing the halides from the tin(IV) compound. For example, with $SnMeCl_3$, the species $[(\mathbf{1})SnMeCl]^{2+}$ with half-integral mass at *m*/*z* 836 was the major peak. This likely arises from $[(\mathbf{1})SnMeCl_2]^+$ (*m*/*z* 1707), which was also observed. A similar pattern was evident when **1** is mixed with $SnMe_2Cl_2$, giving $[(\mathbf{1})SnMe_2]^{2+}$ (*m*/*z* 826) and $[(\mathbf{1})SnMe_2Cl]^+$ (*m*/*z* 1687). Accordingly, a mixture of **1** and Me_3SnCl gives $[(\mathbf{1})SnMe_3]^+$ (*m*/*z* 1667) as the sole product. As shown in Fig. 6, the ES mass spectrum of a mixture of **1** with $SnEt_2Cl_2$ gives the analogous peaks, $[(\mathbf{1})SnEt_2]^{2+}$ (*m*/*z* 840) and $[(\mathbf{1})SnEt_2Cl]^+$ (*m*/*z* 1715). The other related tin(IV) derivatives gave similar patterns (Table 5). These observations demonstrate that, like Au^{III}, Sn at its highest oxidation state is sustainable by the sulfur donors in **1**. To verify the synthetic utility of this unexpected observation, we have synthesized and characterized **5**–**9**, and carried out single-crystal X-ray analyses of the aggregates $[(Ph_3P)_4Pt_2(\mu_3\text{-}S)_2SnMeCl_2]^+$ **5a**, $[(Ph_3P)_4Pt_2(\mu_3\text{-}S)_2\text{-}SnMe_2Cl]^+$ **5b**, $[(Ph_3P)_4Pt_2(\mu_3\text{-}S)_2SnPhCl_2]^+$ **8a**, and $[(Ph_3P)_4\text{-}Pt_2(\mu_3\text{-}S)_2Sn(CH_2Ph)_2Br]^+$ **9**.

(2) Synthesis and structure of the monoprotonated derivative of 1, $[(Ph_3P)_4Pt_2(\mu\text{-}S)(\mu\text{-}SH)][PF_6]$ 2

Based on the ESMS data observed, we have briefly communicated[25] the possible isolability of **2** through careful protonation of **1** by controlling the amount of HCl added to the reaction *via* titration. The ^1H NMR spectrum revealed a peak at δ_H 3.48 corresponding to the lone μ-SH proton. The downfield shift (*cf.* δ_H(RSH) 1.2–1.7) is consistent with the electron withdrawing effect of the $\{Pt_2S_2\}$ ring.[31] The ^{31}P NMR spectrum gives two distinct phosphine environments ($^1J_{Pt-P(1)}$ = 2705 and $^1J_{Pt-P(2)}$ = 3582 Hz). The μ-SH group is expected to be more electron withdrawing (*i.e.* a weaker Lewis base) than the unprotonated μ-S ligand. Hence, the phosphine ligand *trans* to the μ-SH should be manifest as a higher $^1J_{Pt-P(2)}$ value of 3582 Hz while the $^1J_{Pt-P(1)}$ value (2705 Hz) of the phosphine *trans*

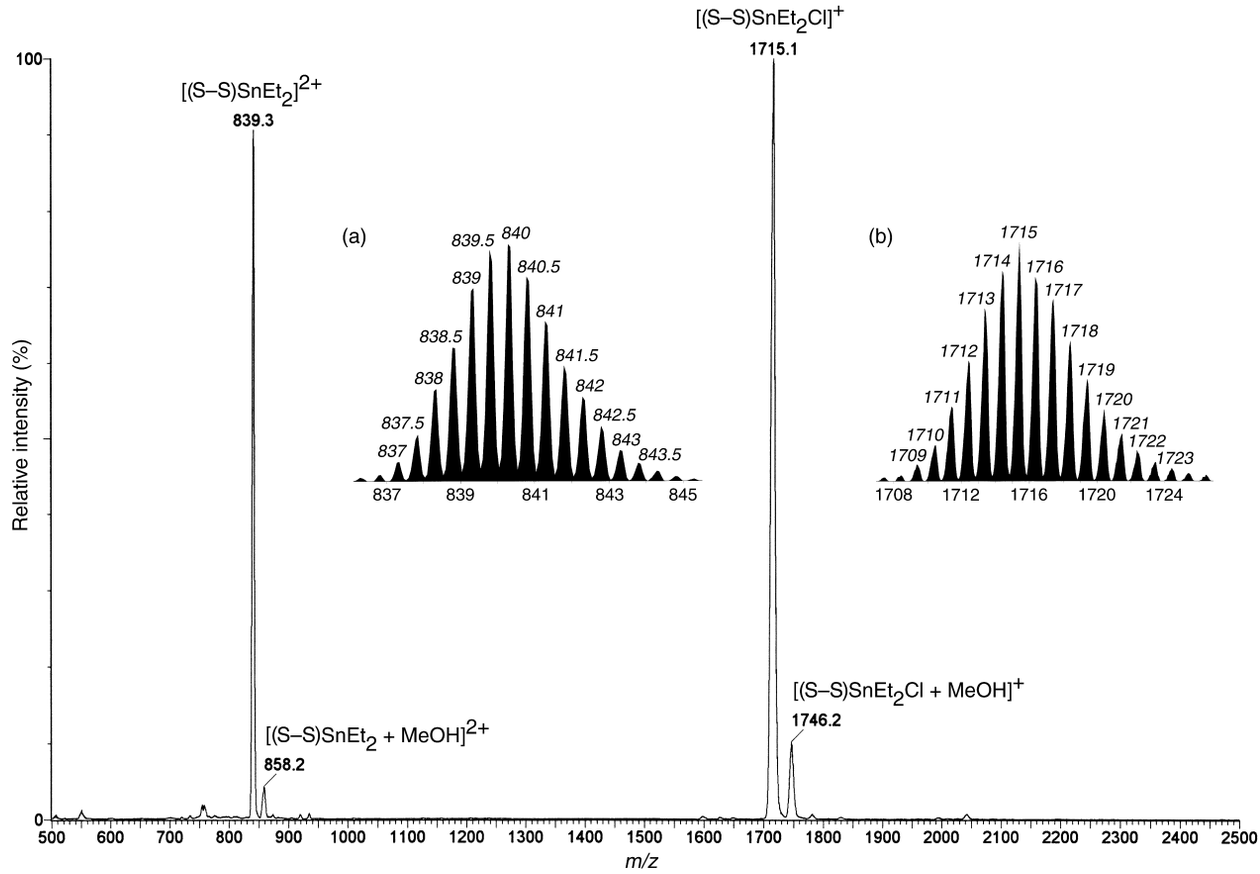

Fig. 6 Positive ion electrospray mass spectrum of an approx. 1 : 1 mixture of **1** with $SnEt_2Cl_2$ in MeOH recorded at a cone voltage of 20 V. The insets show the observed isotope distribution patterns for the ions: (a) $[(\mathbf{1})SnEt_2]^{2+}$ and (b) $[(\mathbf{1})SnEt_2Cl]^{+}$.

to the unprotonated μ-S ligand is indeed very close to that observed for complex **1** in $CDCl_3$ [δ_P 28.03 ($^1J_{Pt-P}$ = 2787 Hz)]. Structurally, complex **2** was analyzed using single crystal X-ray diffraction and revealed a dihedral angle (θ) of 135° which is larger than that of $Pt_2(PMe_2Ph)_4(\mu\text{-}S)_2$ (121°).[32] These suggest that the folding of the $\{Pt_2S_2\}$ core is electronic rather than steric in origin.

(3) Syntheses and structures of organomercury(II) aggregates of $Pt_2(PPh_3)_4(\mu\text{-}S)_2$ 1

Following up on the ESMS evidence, we have synthesized $[(Ph_3P)_4Pt_2(\mu_3\text{-}S)_2HgPh]^+$ **3a** (Fig. 7) and $[(Ph_3P)_4Pt_2(\mu_3\text{-}S)_2\text{-}HgEt]^+$ **3b**, respectively, from stoichiometric reactions of **1** with HgPhCl and Thiomersal in MeOH. The structure shows a bicapped $\{HgPt_2\}$ triangle; the local geometries of the Hg atom is best described as "T shaped". The mercury fragment is asymmetrically disposed with respect to the sulfides. In **3a′** the Hg–S(1) bond distance of 2.9286(12) Å is 21.6% longer than the Hg–S(2) bond distance of 2.4079(12) Å. The "T-shaped" coordination is especially apparent when one of the C–Hg–S angles is nearly linear [C(1)–Hg–S(2) 174.59(16)°]. This contrasts other "Y-shaped" $\{MPt_2S_2\}$ complexes such as $[(Ph_3P)_4Pt_2(\mu_3\text{-}S)_2Cu(PPh_3)][PF_6]$ [P(3)–Cu(3)–S(1) 135.7(2) and P(3)–Cu(3)–S(2) 139.4(4)°].[11] The asymmetric disposition of the Hg atom in **3a′** gives significantly different Hg···Pt distances [3.078(1) and 3.515(1) Å]. This again contrasts that of the isoelectronic gold(I) complexes like $[\{Pt_2(PPh_3)_4(\mu_3\text{-}S)_2\}(AuCl)_2]$ [3.111(1) and 3.218(1) Å] and $[(Ph_3P)_4Pt_2(\mu_3\text{-}S)_2Au(PPh_3)]^+$ [3.314(1) and 3.231(1) Å].[8] Other structural parameters are compared in Table 6.

(4) Syntheses and structures of organogold(III) aggregates of $Pt_2(PPh_3)_4(\mu\text{-}S)_2$ 1

While heterometallic complexes[33] and clusters[34] involving

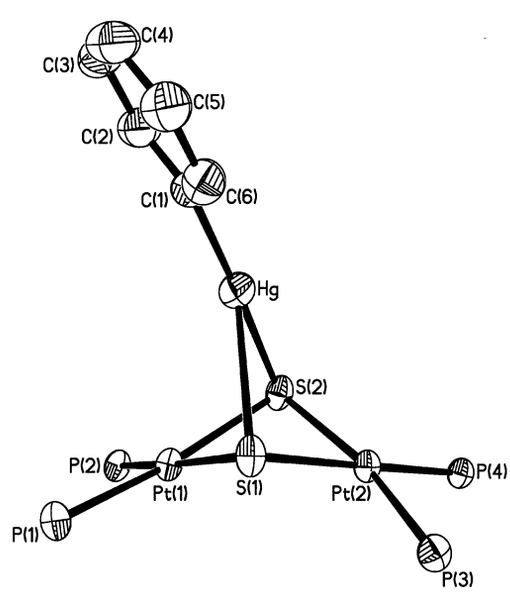

Fig. 7 A 50% thermal ellipsoid representation of $[(Ph_3P)_4Pt_2(\mu_3\text{-}S)_2\text{-}HgPh][BPh_4]$ **3a′** from X-ray coordinates. The phenyl rings of PPh_3 have been omitted for clarity.

gold(I) are commonplace, those containing gold(III) remain scarce, especially those with soft donors like sulfur. Platinum–gold and palladium–gold phosphine cluster compounds have varied applications in catalysis.[35] To our knowledge, reported herein are the first examples of heterometallic Pt^{II}–Au^{III} sulfide aggregates. Complexes of Au^{III}, being isoelectronic with Pd^{II} and Pt^{II} (d^8), display invariably square planar coordination. Similar all-square-planar M_3 aggregates have been reported[24b] but this is the first one involving Au^{III}. Reaction of *cis*-$Au^{III}Cl_2(L_2)$ with **1** gives $[(\mathbf{1})Au^{III}L_2]^{2+}$. Herein we describe the

Table 6 A comparison of selected structural parameters (distances in Å, angles in °) of the heterometallic adducts of **1**

Complex	Heterometal[a] ion M	Coordination geometry of M	Pt · · · Pt	S · · · S	Dihedral angle,[b] θ/°	M · · · Pt	S–M–S	M–S	Ref.
$[(Ph_3P)_4Pt_2(\mu\text{-}S)(\mu\text{-}SH)]^+$ **2**	H^+	Bridging SH	3.340	2.976	135.0	—	—	—	25
$[(Ph_3P)_4Pt_2(\mu_3\text{-}S)_2HgPh]^+$ **3a**′	Hg^{2+}	"T Shaped"	3.268	3.122	132.9	3.078	70.85(3)	2.4709(12)	This work
						3.515		2.9286(12)	
$[(Ph_3P)_4Pt_2(\mu_3\text{-}S)_2Au(pap\text{-}C^1,N)]^{2+}$ **4a**	Au^{3+}	Square planar	3.268	2.968	125.8	3.099	77.28(14)	2.386(4)	This work
						3.196		2.366(4)	
$[(Ph_3P)_4Pt_2(\mu_3\text{-}S)_2Au(tolpy\text{-}C^3,N)]^{2+}$ **4d**	Au^{3+}	Square planar	3.288	2.984	126.8	3.119	78.52(7)	2.335(2)	25
						3.127		2.381(2)	
$[(Ph_3P)_4Pt_2(\mu_3\text{-}S)_2SnMeCl_2]^+$ **5a**	Sn^{4+}	Distorted square-based pyramidal	3.288	3.015	129.4	3.106	72.07(5)	2.5124(16)	This work
						3.446		2.6114(15)	
$[(Ph_3P)_4Pt_2(\mu_3\text{-}S)_2SnMe_2Cl]^+$ **5b**	Sn^{4+}	Distorted trigonal bipyramidal	3.372	2.998	134.7	3.193	70.47(10)	2.643(4)	This work
						3.380		2.552(5)	
$[(Ph_3P)_4Pt_2(\mu_3\text{-}S)_2SnPhCl_2]^+$ **8a**	Sn^{4+}	Distorted square-based pyramidal	3.246	3.030	127.5	3.031	73.35(10)	2.515(3)	This work
						3.457		2.559(3)	
$[(Ph_3P)_4Pt_2(\mu_3\text{-}S)_2Sn(CH_2Ph)_2Br]^+$ **9**	Sn^{4+}	Distorted trigonal bipyramidal	3.263	3.026	126.2	3.353	69.70(10)	2.524(4)	This work
						3.466		2.761(3)	

[a] Except complex **2**. [b] Dihedral angle between two $\{PtS_2\}$ planes.

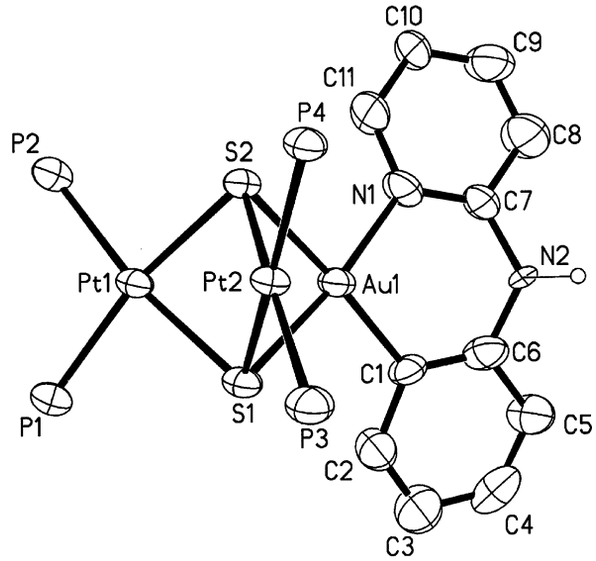

Fig. 8 Structural drawing of $[(Ph_3P)_4Pt_2(\mu_3\text{-}S)_2Au(pap\text{-}C^1,N)][BF_4]_2$ **4a**, with thermal ellipsoids at the 50% probability level. The phenyl rings of PPh_3 have been omitted for clarity.

synthesis and characterization of four such aggregates (see Scheme 4): $[(Ph_3P)_4Pt_2(\mu_3\text{-}S)_2Au(pap\text{-}C^1,N)]^{2+}$ **4a**, $[(Ph_3P)_4Pt_2(\mu_3\text{-}S)_2Au(2\text{-}thpy\text{-}C^3,N)]^{2+}$ **4b**, $[(Ph_3P)_4Pt_2(\mu_3\text{-}S)_2Au(3\text{-}thpy\text{-}C^2,N)]^{2+}$ **4c**, and $[(Ph_3P)_4Pt_2(\mu_3\text{-}S)_2Au(tolpy\text{-}C^3,N)]^{2+}$ **4d**. As previously reported, the solid-state structure confirmed **4d** as $[(Ph_3P)_4Pt_2(\mu_3\text{-}S)_2Au(tolpy\text{-}C^3,N)][BF_4]_2$.[25] This complex showed a square-planar, 16-electron Au^{III} coordinated to both sulfides whilst chelated by a cycloaurated 5-membered ring of the 4-(2-pyridyl)-3-tolyl (**4d**) ligands. Similarly, complex **4a** (Fig. 8) shows a 6-membered ring of the (2-pyridylamino)-phenyl chelating the Au^{III}. In **4d** the presence of the methyl group in the 4-(2-pyridyl)-3-tolyl (tolpy) ligand allowed for unambiguous assignment of N(1) and C(1). In both complexes the $\{Pt_2S_2\}$ rings are puckered [125.8 (**4a**) and 126.8° (**4d**)] with comparable average Au–S bond distances of 2.376(4) (**4a**) and 2.358(2) Å (**4d**). The small dihedral angles between the planes N–Au–C · · · S–Au–S [0.6 (**4a**) and 3.6° (**4d**)] confirm the square disposition of the Au^{III}. The metals are within close proximity (average Pt · · · Au 3.135 Å; Pt · · · Pt 3.278 Å) but non-bonding.

(5) Syntheses and structures of organotin(IV) aggregates of $Pt_2(PPh_3)_4(\mu\text{-}S)_2$ 1

The observation of many heterometallic $\{SnPt_2S_2\}$ species in the ESMS spectra prompted us to undertake a structural study through single crystal X-ray diffraction analyses of the following species: $[(Ph_3P)_4Pt_2(\mu_3\text{-}S)_2SnMeCl_2]^+$ **5a** (Fig. 9), $[(Ph_3P)_4Pt_2(\mu_3\text{-}S)_2SnMe_2Cl]^+$ **5b** (Fig. 10), $[(Ph_3P)_4Pt_2(\mu_3\text{-}S)_2SnPhCl_2]^+$ **8a** (Fig. 11), and $[(Ph_3P)_4Pt_2(\mu_3\text{-}S)_2Sn(CH_2Ph)_2Br]^+$ **9** (Fig. 12) to investigate the preferred geometry of Sn^{IV} in these aggregates. A further impetus was drawn from the relative novelty of heterometallic {SnPtS} complexes, with only one example currently known in the literature, *viz.* $[PtMe_2(Me_2SnS)_2\{(t\text{-}Bu)_2bpy\}]$ [$(t$-Bu)$_2$bpy = 4,4′-di-*tert*-butyl-2,2′-bipyridine].[36] Through this study it is evident that organotin(IV) complexes invariably form five-coordinate aggregates with **1**. In each of these complexes the local coordination geometry at the central Sn^{IV} is largely dependent upon the requirements of the supporting ligands, with both distorted square-based pyramidal or trigonal bipyramidal coordination modes possible.

Another interesting feature of this series of $\{Sn^{IV}Pt_2S_2\}$ aggregates lies in their observed $^1J_{Pt\text{–}P}$ values which decrease in the order: $RSnCl_2^+$ (≈3170) > R_2SnCl^+ (≈3100) > R_3Sn^+ (≈3000 Hz). More specifically, for the series of $[(Ph_3P)_4Pt_2(\mu_3\text{-}S)_2SnR_nX_{(3-n)}]^+$, the following observations are made:

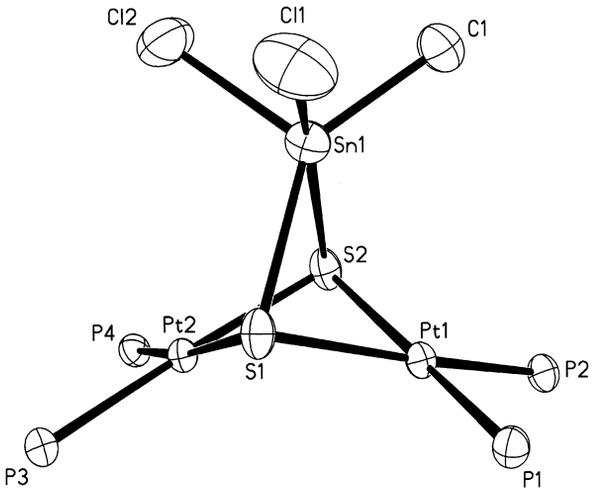

Fig. 9 A 50% thermal ellipsoid representation of $[(Ph_3P)_4Pt_2(\mu_3\text{-}S)_2SnMeCl_2][PF_6]$ **5a** from X-ray coordinates. The phenyl rings of PPh_3 have been omitted for clarity.

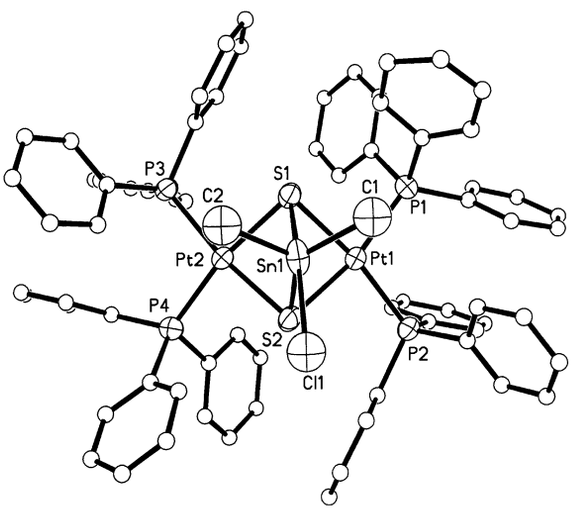

Fig. 10 A 50% thermal ellipsoid representation of $[(Ph_3P)_4Pt_2(\mu_3\text{-}S)_2SnMe_2Cl][PF_6]$ **5b**.

when $n = 1$, $[(Ph_3P)_4Pt_2(\mu_3\text{-}S)_2SnMeCl_2]^+$ **5a** ($^1J_{Pt-P} = 3170$ Hz), $[(Ph_3P)_4Pt_2(\mu_3\text{-}S)_2Sn(n\text{-}Bu)Cl_2]^+$ **7a** ($^1J_{Pt-P} = 3170$ Hz), $[Pt_2(PPh_3)_4(\mu_3\text{-}S)_2SnPhCl_2]^+$ (**8a**; $^1J_{Pt-P} = 3178$ Hz); $n = 2$, $[(Ph_3P)_4Pt_2(\mu_3\text{-}S)_2SnMe_2Cl]^+$ **5b** ($^1J_{Pt-P} = 3109$ Hz), $[(Ph_3P)_4Pt_2(\mu_3\text{-}S)_2SnEt_2Cl]^+$ **6** ($^1J_{Pt-P} = 3109$ Hz), $[(Ph_3P)_4Pt_2(\mu_3\text{-}S)_2Sn(n\text{-}Bu)_2Cl]^+$ **7b** ($^1J_{Pt-P} = 3090$ Hz), $[(Ph_3P)_4Pt_2(\mu_3\text{-}S)_2SnPh_2Cl]^+$ **8b** ($^1J_{Pt-P} = 3128$ Hz), $[(Ph_3P)_4Pt_2(\mu_3\text{-}S)_2Sn(CH_2Ph)_2Br]^+$ **9** ($^1J_{Pt-P} = 3094$ Hz); $n = 3$, $[(Ph_3P)_4Pt_2(\mu_3\text{-}S)_2SnMe_3]^+$ **5c** ($^1J_{Pt-P} = 3002$ Hz), $[(Ph_3P)_4Pt_2(\mu_3\text{-}S)_2SnPh_3]^+$ **8c** ($^1J_{Pt-P} = 3071$ Hz). These variations in the $^1J_{Pt-P}$ values may be rationalized by considering that the Lewis acidity decreases in the order: $RSnCl_2^+ > R_2SnCl^+ > R_3Sn^+$. Hence, the $RSnCl_2^+$ group is expected to be the most electron withdrawing when coordinated to the di-μ-S ligands. This effect causes a stronger coordination of the phosphine ligands to the Pt, and is thus accompanied by concomitantly higher $^1J_{Pt-P}$ values.

Concluding remarks

The chemistry of the $Pt_2L_4(\mu\text{-}S)_2$ core, first reported by Chatt and Mingos (L = $PPhMe_2$)[32] and Ugo *et al.* (L = PPh_3, **1**),[37] and related complexes with the $\{Pt_2Se_2\}$, $\{Pd_2S_2\}$, and $\{Pd_2Se_2\}$ cores represent a unique chapter in coordination chemistry and in the chemistry of heterometallic aggregates and clusters. The nucleophilicity of the hinged di-μ-sulfides or di-μ-selenides favors the synthesis of many intermetallic

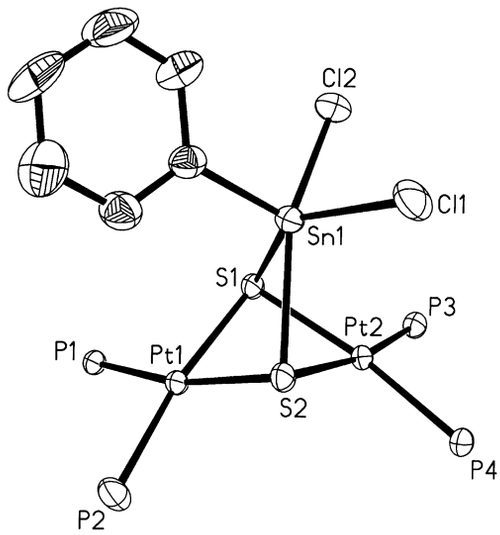

Fig. 11 Structural drawing of $[(Ph_3P)_4Pt_2(\mu_3\text{-}S)_2SnPhCl_2][PF_6]$ **8a** with thermal ellipsoids at the 50% probability level. The phenyl rings of PPh_3 have been omitted for clarity.

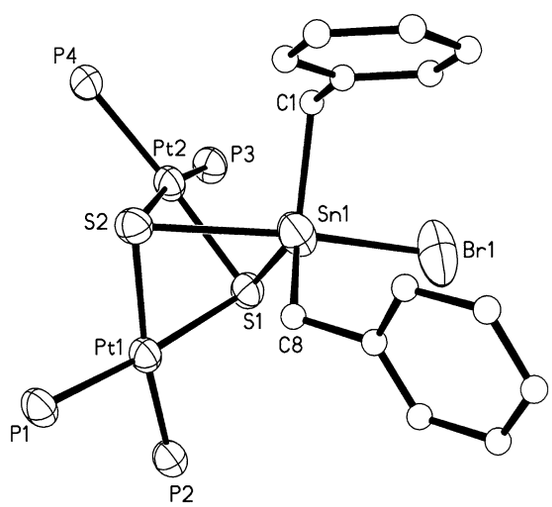

Fig. 12 Structural drawing of $[(Ph_3P)_4Pt_2(\mu_3\text{-}S)_2Sn(CH_2Ph)_2Br][PF_6]$ **9**. Details as in Fig. 11.

aggregates, with ample examples from throughout the Periodic Table.

With the present work based on this ESMS-assisted study of the $\{Pt_2S_2\}$ core a more predictive synthesis approach is spawned. This would greatly help to design synthetic experiments that have a higher chance to yield sustainable multiheterometallic aggregates. The successful synthesis of many of these ESMS active species in our laboratory reinforces this point. Similar approaches can be adopted for other species. For example, aggregates based on $Pt_2(PPh_3)_4(\mu\text{-}Se)_2$[38] have successfully been synthesized.[39] The utility of this strategy for other Lewis acid–base additions would help researchers to search for materials using an approach that is reminiscent of combinatorial chemistry.

In the course of investigating the correlation between observations under ESMS conditions and in the synthetic laboratory, syntheses of mercury(II) (**3**), gold(III) (**4**), and tin(IV) (**5**–**9**) aggregates have been developed, and structural characterization by X-ray diffraction has been achieved for selected entities. We have also recently conducted an electrochemical study of complexes **3a** and **3b** and have encountered some interesting and intricate redox chemistry for these aggregates, which reveals the possible formation of conducting inorganic polymeric films. This will be the subject of an ensuing paper.

Experimental

Electrospray mass spectrometry

Mass spectra were recorded in the positive ion mode using a VG Platform II mass spectrometer at the University of Waikato. MeOH was used as the mobile phase because of the solubility of the ionic species formed in this solvent unless otherwise stated. The spectrometer employed a quadrupole mass filter with an *m*/*z* range of 0–3000. The compounds were dissolved in the mobile phase to give a solution typically of approximate concentration 0.1 mmol L^{-1}, and spectra were recorded for freshly prepared solutions. The dilute sample solution was injected into the spectrometer *via* a Rheodyne injector fitted with a 10 μL sample loop. A Thermo Separation Products Spectra System P1000 LC pump delivered the solution to the mass spectrometer source (maintained at 60 °C) at a flow rate of 20 μL min^{-1}, and nitrogen was employed as both drying and nebulizing gas. Cone voltages were varied from +20 to +180 V in order to investigate the effect of higher voltages on the fragmentation of selected intact gas-phase ions, called precursors in the remainder of this paper. Confirmation of species was aided by comparison of the observed and predicted isotope distribution patterns. Theoretical isotope distribution patterns were calculated using the Isotope computer program[23] and species were identified by the *m*/*z* value of the major peak in their respective isotope distribution pattern.

Materials

The following complexes were prepared by their respective literature procedures, or minor modifications thereof: $AuCl(PPh_3)$,[40] $AuCl(2\text{-}NC_5H_4PPh_2)$,[41] AuCl(tht),[42] $AuCl_2$-(pap-C^1,N),[30c,43] $AuCl_2$(2-thpy-C^3,N),[30b] $AuCl_2$(3-thpy-C^2,N),[30b] $AuCl_2$(tolpy-C^3,N),[29] $Fe(\eta^5\text{-}C_5H_5)(\eta^5\text{-}C_5H_4HgCl)$,[44] $Fe(\eta^5\text{-}C_5H_4HgCl)_2$,[44] $HgCl(C_6H_4CH_2NMe_2\text{-}C^2,N)$,[45] HgCl-(4-$MeOC_6H_3CH_2NMe_2$-$C^2$,$N$),[45] $HgCl_2(PPh_3)_2$,[46] $HgBr_2$-(dppe).[47] $EtHgSC_6H_4CO_2^-Na^+$ (Thiomersal) and HgPhCl were purchased from BDH Chemicals. All 2,4-pentanedionato-O,O' complexes were synthesized *via* the published literature methods: *viz.* $Al(acac)_3$,[48] $VO(acac)_2$,[49] $Cr(acac)_3$,[50] $Mn(acac)_3$,[51] $Fe(acac)_3$,[52] and $Co(acac)_3$.[53] The tin substrates used for this work include $SnMeCl_3$, $SnMe_2Cl_2$, $SnMe_3Cl$, $SnEt_2Cl_2$, Sn(*n*-Bu)Cl_3, Sn(*n*-Bu)$_2Cl_2$, $SnPhCl_3$, $SnPh_2Cl_2$, $SnPh_3Cl$ and $Sn(PhCH_2)_2Cl_2$, all commercially available from Strem Chemicals, Inc. except for $SnEt_2Cl_2$[54] and $Sn(PhCH_2)_2Br_2$.[55]

Unless stated otherwise, all operations were performed using standard Schlenk techniques under an argon atmosphere. $Pt_2(PPh_3)_4(\mu\text{-}S)_2$ **1** was prepared according to the literature method[37] from *cis*-$PtCl_2(PPh_3)_2$ and $Na_2S{\cdot}9H_2O$ in benzene. Solvents used were of reagent grade, dried by published procedures[56] and freshly distilled and degassed under argon prior to use. All other reagents were commercial products used as received. ^1H and $^{31}P\text{-}\{^1H\}$ NMR spectra were recorded on a Bruker ACF 300 MHz spectrometer at *ca.* 300 K at field strengths of 300.0 and 121.5 MHz, respectively. ^1H and ^{31}P chemical shifts are quoted in ppm downfield of $SiMe_4$ and externally referenced to 85% H_3PO_4, respectively. Elemental analyses were performed by the Microanalytical Laboratory, Department of Chemistry, National University of Singapore.

Syntheses of Pt–S–M aggregates (M = H, Hg, Au or Sn)

$[Pt_2(PPh_3)_4(\mu\text{-}S)(\mu\text{-}SH)][PF_6]$ 2. A standard 0.02 M solution of HCl (3.4 mL, 0.0680 mmol) was carefully titrated into an orange suspension of compound **1** (102.0 mg, 0.0678 mmol) in MeOH (40 mL) in a 100 mL Schlenk tube containing a stir bar. The orange suspension turned into a clear yellow solution immediately. After allowing the mixture to stir under an atmosphere of argon for 8 h, a clear, yellow solution was obtained. The mixture was then filtered through Celite; the filter cake and Celite were washed with MeOH (2 × 5 mL) until the washings were colorless. The orange washings and filtrate were combined (50 mL), and an excess of solid NH_4PF_6 (20 mg, 0.1226 mmol) was added. After stirring for 1 h a yellow solid precipitated. Distilled water (10 mL) was then added to induce complete precipitation. The yellow solid was collected on a fine glass frit, washed successively with distilled water (2 × 10 mL), ethanol (5 mL), diethyl ether (10 mL), recrystallized from CH_2Cl_2/*n*-hexane, and dried *in vacuo*, affording a yellow powder of **2** (102.7 mg, 91.8%). Calc. for $C_{73}H_{62.50}Cl_2F_6P_5Pt_2S_2$: C, 52.4; H, 3.7; P, 9.4. Found: C, 52.4; H, 3.6; P, 9.4%. $^{31}P\text{-}\{^1H\}$ NMR ($CDCl_3$): $\delta_{P(1)}$ 20.19 ($^1J_{Pt\text{–}P(1)}$ = 2705, $^2J_{P(1)\text{–}P(2)}$ = 15); $\delta_{P(2)}$ 23.02 ($^1J_{Pt\text{–}P(2)}$ = 3582, $^2J_{P(1)\text{–}P(2)}$ = 15 Hz). ^1H NMR ($CDCl_3$): δ_H 3.48 (s, 1 H, μ-SH), and 7.05–7.45 (m, 60 H, 12 C_6H_5).

$[(Ph_3P)_4Pt_2(\mu_3\text{-}S)_2HgPh][X]$ [X = PF_6 3a or BPh_4 3a′]. A white powder of HgPhCl (10.4 mg, 0.0333 mmol) was added to a 100 mL Schlenk tube containing a rapidly stirred orange suspension of complex **1** (50.1 mg, 0.0333 mmol) in MeOH (20 mL) under an atmosphere of argon. A yellow suspension was formed immediately and stirring was continued for 24 h, at which time a clear, intensely yellow solution was obtained. The mixture was then filtered through Celite; the filter cake and Celite were washed with MeOH (2 × 5 mL) until the washings were colorless. The yellow washings and filtrate were combined (30 mL). Excess of solid NH_4PF_6 (10 mg, 0.0613 mmol) and excess of $NaBPh_4$ (25 mg, 0.0731 mmol) were added to obtain **3a** and **3a′**, respectively. After stirring for 1 h a yellow solid precipitated. Distilled water (10 mL) was then added to promote complete precipitation. The yellow solids were collected on a fine glass frit, washed successively with distilled water (2 × 10 mL), ethanol (5 mL), ether (10 mL), and dried *in vacuo*, affording a yellow powder of **3a** (50.4 mg, 78.6%) and **3a′** (42.1 mg, 60.2%). Calc. for $C_{78}H_{65}F_6HgP_5Pt_2S_2$ **3a**: C, 48.6; H, 3.4; P, 8.0. Found: C, 48.6; H, 3.4; P, 8.1%. $^{31}P\text{-}\{^1H\}$ NMR ($CDCl_3$): δ_P 20.63 ($^1J_{Pt\text{–}P}$ = 3037 Hz). ^1H NMR ($CDCl_3$): δ_H 7.04–7.27 (m, 60 H, 12 C_6H_5), and 7.36–7.44 (m, 5 H, Hg–C_6H_5).

$[(Ph_3P)_4Pt_2(\mu_3\text{-}S)_2HgEt][PF_6]$ 3b. A similar procedure to that described above using a white powder of $EtHgSC_6H_4CO_2^-Na^+$ (Thiomersal) (13.4 mg, 0.0331 mmol) and complex **1** (49.8 mg, 0.0331 mmol) gave a yellow powder of **3b** (48.3 mg, 77.6%) upon addition of excess of NH_4PF_6 (10 mg, 0.0613 mmol). Calc. for $C_{74}H_{65}F_6HgP_5Pt_2S_2$: C, 47.3; H, 3.5; P, 8.2. Found: C, 47.3; H, 3.4; P, 8.1%. $^{31}P\text{-}\{^1H\}$ NMR ($CDCl_3$): δ_P 21.23 ($^1J_{Pt\text{–}P}$ = 3006 Hz). ^1H NMR ($CDCl_3$): δ_H 1.36 (t, 3 H, CH_3), 1.78 (q, 2 H, CH_2), and 7.04–7.75 (m, 60 H, 12 C_6H_5).

$[(Ph_3P)_4Pt_2(\mu_3\text{-}S)_2Au(pap\text{-}C^1,N)][BF_4]_2$ 4a. Similarly, yellow crystals of [$AuCl_2$(pap-C^1,N)] (14.5 mg, 0.0331 mmol), complex **1** (49.8 mg, 0.0331 mmol) and excess of NH_4BF_4 (10 mg, 0.0954 mmol) gave a light yellow powder of **4a** (50.9 mg, 75.2%). Calc. for $C_{83}H_{69}AuB_2F_8N_2P_4Pt_2S_2$: C, 48.8; H, 3.4; P, 6.1. Found: C, 49.0; H, 3.5; P, 6.0%. $^{31}P\text{-}\{^1H\}$ NMR ($CDCl_3$): δ_P 14.91 ($^1J_{Pt\text{–}P}$ = 3197 Hz). ^1H NMR ($CDCl_3$): δ_H 3.68 (s, 1 H, N–H), 5.70–6.50 (m, 4 H, anilino H), 7.17–7.35 (m, 60 H, 12 C_6H_5), and 7.56–9.61 (m, 4 H, pyridyl H).

Isomeric $[(Ph_3P)_4Pt_2(\mu_3\text{-}S)_2Au(2\text{-}thpy\text{-}C^3,N)][PF_6]_2$ 4b and $[(Ph_3P)_4Pt_2(\mu_3\text{-}S)_2Au(3\text{-}thpy\text{-}C^2,N)][PF_6]_2$ 4c. In analogous and parallel procedures, complex **1** (100.0 mg, 0.0664 mmol) with pale green crystals of [$AuCl_2$(2-thpy-C^3,N)] (28.4 mg, 0.0664 mmol) and **1** (100.0 mg, 0.0664 mmol) with orange crystals of [$AuCl_2$(3-thpy-C^2,N)] (28.4 mg, 0.0664 mmol), together with excess of NH_4PF_6 (30 mg, 0.1840 mmol) gave a light yellow powder of **4b** (101.8 mg, 71.2%) and a yellow powder of **4c** (104.8 mg, 73.3%), respectively. Calc. for $C_{81}H_{66}AuF_{12}NP_6Pt_2S_3$: C, 45.2; H, 3.1; P, 8.6. Found: **4b** C, 45.0; H, 3.1; P, 8.4. **4c** C, 45.1; H, 3.0; P, 8.5%. $^{31}P\text{-}\{^1H\}$ NMR (CD_2Cl_2): **4b** $\delta_{P(1)}$ 14.55 ($^1J_{Pt\text{–}P(1)}$ = 3201, $^2J_{P(1)\text{–}P(2)}$ = 8) and $\delta_{P(2)}$ 15.29 ($^1J_{Pt\text{–}P(2)}$ = 3311,

Table 7 Selected bond distances (Å) and bond angles (°) for complexes **3a′**, **4a**, **5a**, **5b**, **8a** and **9**

$[(Ph_3P)_4Pt_2(\mu_3\text{-}S)_2HgPh][BPh_4]\cdot 2CH_2Cl_2$, **3a′**

Pt(1)–S(1)	2.3460(11)	Pt(1)–S(2)	2.4077(11)	Pt(2)–S(1)	2.3560(11)	Pt(2)–S(2)	2.3684(11)
Hg–S(1)	2.9286(12)	Hg–S(2)	2.4079(12)	Pt(1)–P(1)	2.2701(12)	Pt(1)–P(2)	2.2951(11)
Pt(2)–P(3)	2.2909(12)	Pt(2)–P(4)	2.3020(11)	Hg–C(1)	2.081(5)		
P(1)–S(1)–Pt(2)	88.05(4)	Pt(1)–S(2)–Pt(2)	86.34(4)	Pt(1)–S(1)–Hg	70.41(3)	Pt(1)–S(2)–Hg	79.46(3)
Pt(2)–S(1)–Hg	82.62(3)	Pt(2)–S(2)–Hg	94.77(4)	S(1)–Pt(1)–S(2)	82.10(4)	S(1)–Pt(2)–S(2)	82.73(4)
P(1)–Pt(1)–P(2)	98.64(4)	P(3)–Pt(2)–P(4)	99.79(4)	P(1)–Pt(1)–S(1)	91.06(4)	P(3)–Pt(2)–S(1)	85.16(4)
P(1)–Pt(1)–S(2)	170.03(4)	P(3)–Pt(2)–S(2)	167.22(4)	S(1)–Hg–S(2)	70.85(3)	C(1)–Hg–S(1)	113.00(15)
C(1)–Hg–S(2)	174.59(16)						

$[(Ph_3P)_4Pt_2(\mu_3\text{-}S)_2Au(pap\text{-}C^1,N)][BF_4]_2\cdot 4.5CH_2Cl_2$, **4a**

Pt(1)–S(1)	2.369(4)	Pt(1)–S(2)	2.342(4)	Pt(2)–S(1)	2.362(4)	Pt(2)–S(2)	2.367(4)
Au(1)–S(1)	2.386(4)	Au(1)–S(2)	2.366(4)	Pt(1)–P(1)	2.296(5)	Pt(1)–P(2)	2.285(5)
Pt(2)–P(3)	2.287(5)	Pt(2)–P(4)	2.295(4)	Au(1)–C(1)	2.039(17)	Au(1)–N(1)	2.075(15)
Pt(1)–S(1)–Pt(2)	87.37(14)	Pt(1)–S(2)–Pt(2)	87.89(14)	Pt(1)–S(1)–Au(1)	84.44(14)	Pt(1)–S(2)–Au(1)	85.49(14)
Pt(2)–S(1)–Au(1)	81.48(13)	Pt(2)–S(2)–Au(1)	81.81(13)	S(1)–Pt(1)–S(2)	78.10(14)	S(1)–Pt(2)–S(2)	77.73(15)
P(1)–Pt(1)–P(2)	99.54(18)	P(3)–Pt(2)–P(4)	98.85(17)	P(1)–Pt(1)–S(1)	89.75(16)	P(3)–Pt(2)–S(1)	93.65(16)
P(1)–Pt(1)–S(2)	167.80(16)	P(3)–Pt(2)–S(2)	170.24(17)	S(1)–Au(1)–S(2)	77.28(14)	C(1)–Au(1)–N(1)	89.6(7)
C(1)–Au(1)–S(1)	98.1(5)	C(1)–Au(1)–S(2)	175.3(5)	N(1)–Au(1)–S(1)	172.3(5)	N(1)–Au(1)–S(2)	95.0(5)

$[(Ph_3P)_4Pt_2(\mu_3\text{-}S)_2SnMeCl_2][PF_6]$, **5a**

Pt(1)–S(1)	2.3622(14)	Pt(1)–S(2)	2.3873(14)	Pt(2)–S(1)	2.3653(14)	Pt(2)–S(2)	2.3339(14)
Sn(1)–S(1)	2.5124(16)	Sn(1)–S(2)	2.6114(15)	Pt(1)–P(1)	2.2833(14)	Pt(1)–P(2)	2.3143(14)
Pt(2)–P(3)	2.3039(14)	Pt(2)–P(4)	2.2814(15)	Sn(1)–Cl(1)	2.425(2)	Sn(1)–Cl(2)	2.3665(19)
Sn(1)–C(1)	2.125(6)						
Pt(1)–S(1)–Pt(2)	88.12(5)	Pt(1)–S(2)–Pt(2)	88.26(5)	Pt(1)–S(1)–Sn(1)	79.09(4)	Pt(1)–S(2)–Sn(1)	76.68(4)
Pt(2)–S(1)–Sn(1)	89.84(5)	Pt(2)–S(2)–Sn(1)	88.16(5)	S(1)–Pt(1)–S(2)	78.82(5)	S(1)–Pt(2)–S(2)	79.83(5)
P(1)–Pt(1)–P(2)	99.62(5)	P(3)–Pt(2)–P(4)	98.28(5)	P(1)–Pt(1)–S(1)	92.49(5)	P(3)–Pt(2)–S(1)	90.07(5)
P(1)–Pt(1)–S(2)	170.14(5)	P(3)–Pt(2)–S(2)	169.89(5)	S(1)–Sn(1)–S(2)	72.07(5)	Cl(1)–Sn(1)–S(1)	88.08(6)
Cl(1)–Sn(1)–Cl(2)	93.85(9)	Cl(2)–Sn(1)–S(1)	114.13(6)	C(1)–Sn(1)–Cl(1)	94.3(2)	C(1)–Sn(1)–S(2)	96.3(2)
C(1)–Sn(1)–Cl(2)	105.3(2)	Cl(1)–Sn(1)–S(2)	158.79(7)	C(1)–Sn(1)–S(1)	140.3(2)	Cl(2)–Sn(1)–S(2)	100.96(6)

$[(Ph_3P)_4Pt_2(\mu_3\text{-}S)_2SnMe_2Cl][PF_6]$, **5b**

Pt(1)–S(1)	2.374(2)	Pt(1)–S(2)	2.350(2)	Pt(2)–S(1)	2.361(2)	Pt(2)–S(2)	2.368(2)
Sn(1)–S(1)	2.643(4)	Sn(1)–S(2)	2.552(5)	Pt(1)–P(1)	2.322(2)	Pt(1)–P(2)	2.300(2)
Pt(2)–P(3)	2.292(2)	Pt(2)–P(4)	2.322(2)	Sn(1)–Cl(1)	2.489(6)	Sn(1)–C(1)	2.153(13)
Sn(1)–C(2)	2.144(13)						
Pt(1)–S(1)–Pt(2)	90.82(7)	Pt(1)–S(2)–Pt(2)	91.26(7)	Pt(1)–S(1)–Sn(1)	78.84(10)	Pt(1)–S(2)–Sn(1)	81.18(10)
Pt(2)–S(1)–Sn(1)	84.80(11)	Pt(2)–S(2)–Sn(1)	86.72(11)	S(1)–Pt(1)–S(2)	78.78(8)	S(1)–Pt(2)–S(2)	78.69(8)
P(1)–Pt(1)–P(2)	100.72(8)	P(3)–Pt(2)–P(4)	98.81(8)	P(1)–Pt(1)–S(1)	89.15(8)	P(3)–Pt(2)–S(1)	91.03(7)
P(1)–Pt(1)–S(2)	167.92(8)	P(3)–Pt(2)–S(2)	168.43(8)	S(1)–Sn(1)–S(2)	70.47(10)	C(1)–Sn(1)–S(1)	100.1(5)
C(1)–Sn(1)–C(2)	107.1(7)	C(2)–Sn(1)–S(1)	98.1(5)	C(1)–Sn(1)–Cl(1)	93.6(5)	Cl(1)–Sn(1)–S(2)	86.6(2)
C(2)–Sn(1)–Cl(1)	95.3(5)	C(1)–Sn(1)–S(2)	131.0(6)	Cl(1)–Sn(1)–S(1)	157.0(2)	C(2)–Sn(1)–S(2)	121.6(6)

$[(Ph_3P)_4Pt_2(\mu_3\text{-}S)_2SnPhCl_2][PF_6]\cdot 2.5CHCl_3$, **8a**

Pt(1)–S(1)	2.344(3)	Pt(1)–S(2)	2.339(3)	Pt(2)–S(1)	2.371(3)	Pt(2)–S(2)	2.389(3)
Sn(1)–S(1)	2.515(3)	Sn(1)–S(2)	2.559(3)	Pt(1)–P(1)	2.307(3)	Pt(1)–P(2)	2.289(4)
Pt(2)–P(3)	2.288(3)	Pt(2)–P(4)	2.323(3)	Sn(1)–Cl(1)	2.389(4)	Sn(1)–Cl(2)	2.414(3)
Sn(1)–C(1M)	2.112(14)						
Pt(1)–S(1)–Pt(2)	87.04(10)	Pt(1)–S(2)–Pt(2)	86.72(10)	Pt(1)–S(1)–Sn(1)	90.65(10)	Pt(1)–S(2)–Sn(1)	89.67(10)
Pt(2)–S(1)–Sn(1)	76.62(8)	Pt(2)–S(2)–Sn(1)	75.45(9)	S(1)–Pt(1)–S(2)	80.65(10)	S(1)–Pt(2)–S(2)	79.09(10)
P(1)–Pt(1)–P(2)	100.85(12)	P(3)–Pt(2)–P(4)	99.61(11)	P(1)–Pt(1)–S(1)	87.13(10)	P(3)–Pt(2)–S(1)	91.43(11)
P(1)–Pt(1)–S(2)	167.39(11)	P(3)–Pt(2)–S(2)	170.15(11)	S(1)–Sn(1)–S(2)	73.35(10)	Cl(1)–Sn(1)–S(1)	139.59(13)
Cl(1)–Sn(1)–Cl(2)	89.16(13)	Cl(2)–Sn(1)–S(1)	88.45(11)	C(1M)–Sn(1)–Cl(1)	106.1(4)	C(1M)–Sn(1)–S(2)	106.4(4)
C(1M)–Sn(1)–Cl(2)	100.1(4)	Cl(1)–Sn(1)–S(2)	91.37(11)	C(1M)–Sn(1)–S(1)	114.0(4)	Cl(2)–Sn(1)–S(2)	152.17(12)

$[(Ph_3P)_4Pt_2(\mu_3\text{-}S)_2Sn(CH_2Ph)_2Br][PF_6]\cdot 0.5CHCl_3$, **9**

Pt(1)–S(1)	2.372(3)	Pt(1)–S(2)	2.370(3)	Pt(2)–S(1)	2.375(3)	Pt(2)–S(2)	2.381(3)
Sn(1)–S(1)	2.524(4)	Sn(1)–S(2)	2.761(3)	Pt(1)–P(1)	2.302(3)	Pt(1)–P(2)	2.333(4)
Pt(2)–P(3)	2.317(3)	Pt(2)–P(4)	2.318(3)	Sn(1)–Br(1)	2.612(2)	Sn(1)–C(1)	2.170(15)
Sn(1)–C(8)	2.161(17)						
Pt(1)–S(1)–Pt(2)	86.87(11)	Pt(1)–S(2)–Pt(2)	86.77(11)	Pt(1)–S(1)–Sn(1)	90.08(11)	Pt(1)–S(2)–Sn(1)	84.62(0)
Pt(2)–S(1)–Sn(1)	86.31(11)	Pt(2)–S(2)–Sn(1)	81.03(9)	S(1)–Pt(1)–S(2)	79.31(11)	S(1)–Pt(2)–S(2)	79.03(11)
P(1)–Pt(1)–P(2)	100.04(12)	P(3)–Pt(2)–P(4)	100.88(13)	P(1)–Pt(1)–S(1)	170.99(13)	P(3)–Pt(2)–S(1)	91.49(12)
P(1)–Pt(1)–S(2)	92.25(12)	P(3)–Pt(2)–S(2)	170.38(12)	S(1)–Sn(1)–S(2)	69.70(10)	C(1)–Sn(1)–S(1)	124.3(5)
C(1)–Sn(1)–C(8)	117.2(7)	C(8)–Sn(1)–S(1)	115.8(5)	C(1)–Sn(1)–Br(1)	94.4(5)	Br(1)–Sn(1)–S(2)	159.08(10)
C(8)–Sn(1)–Br(1)	102.5(5)	C(1)–Sn(1)–S(2)	93.5(5)	Br(1)–Sn(1)–S(1)	89.89(10)	C(8)–Sn(1)–S(2)	90.9(4)

$^2J_{P(1)-P(2)} = 8$); **4c** $\delta_{P(1)}$ 14.13 ($^1J_{Pt-P(1)} = 3223$, $^2J_{P(1)-P(2)} = 8$) and $\delta_{P(2)}$ 15.19 ($^1J_{Pt-P(2)} = 3307$, $^2J_{P(1)-P(2)} = 8$ Hz). ^{1}H NMR (CD_2Cl_2): **4b** δ_H 5.71 (d, 1 H, thienyl H), 6.70 (d, 1 H, thienyl H), 7.09–7.40 (m, 60 H, 12 C_6H_5), 7.50–9.29 (m, 4 H, pyridyl H); **4c** δ_H 6.65 (d, 1 H, thienyl H), 7.05 (d, 1 H, thienyl H), 7.10–7.44 (m, 60 H, 12 C_6H_5), 7.55–9.25 (m, 4 H, pyridyl H).

[$(Ph_3P)_4Pt_2(\mu_3\text{-}S)_2Au$(tolpy-$C^3$,$N$)][$BF_4$]$_2$ 4d. Similarly, yellow crystals of [$AuCl_2$(tolpy-C^3,N)] (14.6 mg, 0.0333 mmol) and complex **1** (50.1 mg, 0.0333 mmol) with excess of NH_4BF_4 (10 mg, 0.0954 mmol) gave a yellow powder of **4d** (56.5 mg, 83.0%). Calc. for $C_{84}H_{70}AuB_2F_8NP_4Pt_2S_2$: C, 49.4; H, 3.5; P, 6.1. Found: C, 49.4; H, 3.4; P, 6.0%. ^{31}P-{^{1}H} NMR ($CDCl_3$): $\delta_{P(1)}$ 14.74 (d, 2 P, 2 PPh_3) ($^1J_{Pt-P(1)} = 3304$, $^2J_{P(1)-P(2)} = 18$); $\delta_{P(2)}$ 14.96 (d, 2 P, 2 PPh_3) ($^1J_{Pt-P(2)} = 3208$, $^2J_{P(1)-P(2)} = 18$ Hz). ^{1}H NMR ($CDCl_3$): δ_H 2.21 (s, 3 H, Me), 5.70–6.83 (m, 3 H, tolyl H), 7.14–7.39 (m, 60 H, 12 C_6H_5), and 7.46–8.37 (m, 4 H, pyridyl H).

[$(Ph_3P)_4Pt_2(\mu_3\text{-}S)_2SnMeCl_2$][$PF_6$] 5a. Colorless crystals of $SnMeCl_3$ (8.0 mg, 0.0333 mmol) were added to a 100 mL Schlenk tube containing a rapidly stirred orange suspension of **1** (50.0 mg, 0.0333 mmol) in MeOH (20 mL) under an atmosphere of argon. A pale yellow solution was formed immediately and stirring continued for 24 h. Addition of excess of NH_4PF_6 (16.3 mg, 0.1000 mmol) yielded a pale yellow suspension that was stirred for 3 h, after which distilled water (60 mL) was added to induce complete precipitation. The suspension was then filtered through a glass frit, and the pale yellow residue thus obtained washed successively with distilled water (2 × 10 mL), minimal ethanol (2 mL), followed by copious amounts of diethyl ether (2 × 20 mL), and dried *in vacuo*, yielding a pale yellow powder of **5a** (36.7 mg, 59.6%). Calc. for $C_{73}H_{63}Cl_2F_6P_5Pt_2S_2Sn$: C, 47.3; H, 3.4; P, 8.4. Found: C, 47.3; H, 3.4; P, 8.5%. ^{31}P-{^{1}H} NMR (CD_2Cl_2): δ_P 15.29 ($^1J_{Pt-P} = 3170$ Hz). ^{1}H NMR (CD_2Cl_2): δ_H 1.32 (s, 3 H, CH_3) and 6.87–7.32 (m, 60 H, 12 C_6H_5).

[$(Ph_3P)_4Pt_2(\mu_3\text{-}S)_2SnMe_2Cl$][$PF_6$] 5b. A similar procedure to that described above using pale yellow crystals of $SnMe_2Cl_2$ (7.3 mg, 0.0333 mmol) and complex **1** (50.0 mg, 0.0333 mmol) gave a pale yellow powder of **5b** (24.2 mg, 39.7%). Calc. for $C_{74}H_{66}ClF_6P_5Pt_2S_2Sn$: C, 48.5; H, 3.6; P, 8.5. Found: C, 48.5; H, 3.5; P, 8.5%. ^{31}P-{^{1}H} NMR ($CDCl_3$): δ_P 16.77 ($^1J_{Pt-P} = 3109$ Hz). ^{1}H NMR ($CDCl_3$): δ_H 1.17 (s, 6 H, 2 CH_3) and 7.12–7.30 (m, 60 H, 12 C_6H_5).

[$(Ph_3P)_4Pt_2(\mu_3\text{-}S)_2SnMe_3$][$PF_6$] 5c. Similarly, pale yellow crystals of $SnMe_3Cl$ (6.6 mg, 0.0333 mmol) and complex **1** (50.0 mg, 0.0333 mmol) gave a pale yellow powder of **5c** (28.9 mg, 48.0%). Calc. for $C_{75}H_{69}F_6P_5Pt_2S_2Sn$: C, 49.7; H, 3.8; P, 8.5. Found: C, 49.7; H, 3.7; P, 8.4%. ^{31}P-{^{1}H} NMR ($CDCl_3$): δ_P 21.92 ($^1J_{Pt-P} = 3002$ Hz). ^{1}H NMR ($CDCl_3$): δ_H 1.26 (s, 9 H, 3 CH_3) and 7.04–7.29 (m, 60 H, 12 C_6H_5).

[$(Ph_3P)_4Pt_2(\mu_3\text{-}S)_2SnEt_2Cl$][$PF_6$] 6. Similarly, colorless crystals of $SnEt_2Cl_2$ (8.2 mg, 0.0333 mmol) and complex **1** (50.0 mg, 0.0333 mmol) gave a pale yellow powder of **6** (16.9 mg, 27.3%). Calc. for $C_{76}H_{70}ClF_6P_5Pt_2S_2Sn$: C, 49.1; H, 3.8; P, 8.3. Found: C, 49.2; H, 3.9; P, 8.3%. ^{31}P-{^{1}H} NMR ($CDCl_3$): δ_P 16.70 ($^1J_{Pt-P} = 3109$ Hz). ^{1}H NMR ($CDCl_3$): δ_H 1.26 (t, 6 H, 2 CH_3), 2.62 (q, 4 H, 2 CH_2) and 7.12–7.31 (m, 60 H, 12 C_6H_5).

[$(Ph_3P)_4Pt_2(\mu_3\text{-}S)_2Sn$(*n*-Bu)$Cl_2$][$PF_6$] 7a. Similarly, the pale yellow liquid Sn(*n*-Bu)Cl_3 (9.4 mg, 5.54 μL, 0.0333 mmol) and complex **1** (50.0 mg, 0.0333 mmol) gave a pale yellow powder of **7a** (26.0 mg, 41.3%). Calc. for $C_{76}H_{69}Cl_2F_6P_5Pt_2S_2Sn$: C, 48.2; H, 3.7; P, 8.2. Found: C, 48.2; H, 3.8; P, 8.1%. ^{31}P-{^{1}H} NMR ($CDCl_3$): δ_P 15.29 ($^1J_{Pt-P} = 3170$ Hz). ^{1}H NMR ($CDCl_3$): δ_H 1.33 (t, 3 H, CH_3), 1.49–1.54 (m, 4 H, 2 CH_2), 1.83 (t, 2 H, CH_2) and 7.11–7.69 (m, 60 H, 12 C_6H_5).

[$(Ph_3P)_4Pt_2(\mu_3\text{-}S)_2Sn$(*n*-Bu)$_2$Cl][$PF_6$] 7b. Similarly, colorless crystals of Sn(*n*-Bu)$_2Cl_2$ (10.1 mg, 0.0333 mmol) and complex **1** (50.0 mg, 0.0333 mmol) gave a pale yellow powder of **7b** (18.5 mg, 29.0%). Calc. for $C_{80}H_{78}ClF_6P_5Pt_2S_2Sn$: C, 50.1; H, 4.1; P, 8.1. Found: C, 50.0; H, 4.1; P, 8.1%. ^{31}P-{^{1}H} NMR ($CDCl_3$): δ_P 16.74 ($^1J_{Pt-P} = 3090$ Hz). ^{1}H NMR ($CDCl_3$): δ_H 1.31 (t, 3 H, CH_3), 1.52–1.61 (m, 4 H, 2 CH_2), 1.90 (t, 2 H, CH_2) and 7.15–7.32 (m, 60 H, 12 C_6H_5).

[$(Ph_3P)_4Pt_2(\mu_3\text{-}S)_2SnPhCl_2$][$PF_6$] 8a. Similarly, a pale yellow liquid $SnPhCl_3$ (10.1 mg, 5.46 μL, 0.0333 mmol) and complex **1** (50.0 mg, 0.0333 mmol) gave a pale yellow powder of **8a** (36.0 mg, 56.5%). Calc. for $C_{78}H_{65}Cl_2F_6P_5Pt_2S_2Sn$: C, 48.9; H, 3.4; P, 8.1. Found: C, 48.8; H, 3.4; P, 8.0%. ^{31}P-{^{1}H} NMR ($CDCl_3$): δ_P 15.20 ($^1J_{Pt-P} = 3178$ Hz). ^{1}H NMR ($CDCl_3$): δ_H 7.07–7.33 (m, 60 H, 12 C_6H_5) and 7.42–7.54 (m, 5 H, SnC_6H_5).

[$(Ph_3P)_4Pt_2(\mu_3\text{-}S)_2SnPh_2Cl$][$PF_6$] 8b. Similarly, white crystals of $SnPh_2Cl_2$ (22.9 mg, 0.0665 mmol) and complex **1** (100.0 mg, 0.0665 mmol) gave a pale yellow powder of **8b** (101.9 mg, 78.3%). Calc. for $C_{84}H_{70}ClF_6P_5Pt_2S_2Sn$: C, 51.6; H, 3.6; P, 7.9. Found: C, 51.5; H, 3.7; P, 7.9%. ^{31}P-{^{1}H} NMR ($CDCl_3$): δ_P 15.45 ($^1J_{Pt-P} = 3128$ Hz). ^{1}H NMR ($CDCl_3$): δ_H 7.05–7.86 (m, 70 H, 14 C_6H_5).

[$(Ph_3P)_4Pt_2(\mu_3\text{-}S)_2SnPh_3$][$PF_6$] 8c. Similarly, white crystals of $SnPh_3Cl$ (12.8 mg, 0.0333 mmol) and complex **1** (50.0 mg, 0.0333 mmol) gave a pale yellow powder of **8c** (29.6 mg, 44.5%). Calc. for $C_{90}H_{75}F_6P_5Pt_2S_2Sn$: C, 54.1; H, 3.8; P, 7.7. Found: C, 54.1; H, 3.7; P, 7.8%. ^{31}P-{^{1}H} NMR ($CDCl_3$): δ_P 20.03 ($^1J_{Pt-P} = 3071$ Hz). ^{1}H NMR ($CDCl_3$): δ_H 6.92–7.72 (m, 75 H, 15 C_6H_5).

[$(Ph_3P)_4Pt_2(\mu_3\text{-}S)_2Sn(CH_2Ph)_2Br$][$PF_6$] 9. Similarly, white crystals of $Sn(PhCH_2)_2Br_2$ (15.3 mg, 0.0333 mmol) and complex **1** (50.0 mg, 0.0333 mmol) gave a pale yellow powder of **9** (12.6 mg, 18.7%). Calc. for $C_{86}H_{74}BrF_6P_5Pt_2S_2Sn$: C, 50.9; H, 3.7; P, 7.6. Found: C, 51.4; H, 3.7; P, 7.7%. ^{31}P-{^{1}H} NMR ($CDCl_3$): δ_P 16.45 ($^1J_{Pt-P} = 3094$ Hz). ^{1}H NMR ($CDCl_3$): δ_H 3.02 (d, 2 H, $PhCH_2$), 3.31 (d, 2 H, $PhCH_2$), 6.42–6.88 (m, 10 H, $C_6H_5CH_2$) and 7.01–7.51 (m, 60 H, 12 C_6H_5).

Crystal structure determination and refinement

The selected bond lengths and angles for **3a′**, **4a**, **5a**, **5b**, **8a**, and **9** are given in Table 7. The intensities of **4a**, **5a**, **5b**, **8a** and **9** were measured at National University of Singapore on a Bruker AXS SMART diffractometer while **3a′** was analyzed at the University of Auckland on a Siemens SMART diffractometer. Each set-up was equipped with a CCD area detector using Mo-Kα radiation ($\lambda = 0.71073$ Å). The software SMART[57] was used for collecting frames of data, indexing reflections, and determination of lattice parameters, SAINT[57] for integration of intensity of reflections and scaling, SADABS[58] for empirical absorption correction, and SHELXTL[59] for space group and structure determination, refinements, graphics, and structure reporting. A summary of crystallographic parameters for the data collections and refinements is given in Table 8.

Suitable single crystals of [$Pt_2(Ph_3P)_4(\mu_3\text{-}S)_2HgPh$][$BPh_4$]·$2CH_2Cl_2$ **3a′** and [$Pt_2(Ph_3P)_4(\mu_3\text{-}S)_2Au$(pap-$C^1$,$N$)][$BF_4$]$_2$·$4.5CH_2Cl_2$ **4a** were obtained by carefully layering ether onto a CH_2Cl_2 solution (2 : 1) at 5 °C. Single crystals of [$(Ph_3P)_4Pt_2(\mu_3\text{-}S)_2SnMeCl_2$][$PF_6$] **5a**, [$(Ph_3P)_4Pt_2(\mu_3\text{-}S)_2SnMe_2Cl$][$PF_6$] **5b**, [$(Ph_3P)_4Pt_2(\mu_3\text{-}S)_2SnPhCl_2$][$PF_6$]·$2.5CHCl_3$ **8a**, [$(Ph_3P)_4Pt_2(\mu_3\text{-}S)_2Sn(CH_2Ph)_2Br$][$PF_6$]·$0.5CHCl_3$ **9** were obtained by carefully layering a $CHCl_3$ solution of each compound with *n*-hexane at 25 °C. The crystals were quickly transferred from the sample vial onto a microscope slide containing Paratone N oil, after which a suitable crystal was selected and quickly mounted on a glass fiber using wax. For **3a′** there were two

Table 8 Crystallographic data for complexes **3a′**, **4a**, **5a**, **5b**, **8a** and **9**

	3a′·$2CH_2Cl_2$	**4a**·$4.5CH_2Cl_2$	**5a**	**5b**	**8a**·$2.5CHCl_3$	**9**·$0.5CHCl_3$
Formula	$C_{104}H_{89}BCl_4HgP_4Pt_2S_2$	$C_{87.5}H_{79}AuB_2Cl_9F_8N_2P_4Pt_2S_2$	$C_{73}H_{63}Cl_2F_6P_5Pt_2S_2Sn$	$C_{74}H_{66}ClF_6P_5Pt_2S_2Sn$	$C_{80.5}H_{67.5}Cl_{9.5}F_6P_5Pt_2S_2Sn$	$C_{86.5}H_{74.5}BrCl_{1.5}F_6P_5Pt_2S_2Sn$
Formula weight	2270.13	2426.34	1852.97	1832.56	2237.46	2088.89
Crystal system	Triclinic	Monoclinic	Monoclinic	Monoclinic	Triclinic	Monoclinic
Space group	$P\bar{1}$	$P2_1/c$	$P2_1/c$	$P2_1/c$	$P\bar{1}$	$P2_1/n$
a/Å	13.6833(2)	26.6932(4)	19.8509(4)	20.0451(2)	13.6794(2)	13.9114(2)
b/Å	17.5864(3)	15.0637(2)	19.3975(4)	19.7353(1)	16.1453(1)	19.3113(2)
c/Å	19.5672(2)	26.8548(4)	17.8759(4)	17.9958(1)	21.8422(1)	32.5520(1)
α/°	82.352(1)	90	90	90	108.994(1)	90
β/°	88.935(1)	109.519(1)	91.769(1)	90.440(1)	91.992(1)	90.743(1)
γ/°	81.599(1)	90	90	90	90.339(1)	90
V/Å^3	4616.69(11)	10177.7(3)	6880.0(3)	7118.86(9)	4563.85(8)	8744.3(2)
Z	2	4	4	4	2	4
μ/mm^{-1}	4.959	4.576	4.731	4.535	3.795	4.171
T/K	200(2)	223(2)	293(2)	293(2)	203(2)	293(2)
Reflections collected	43769	50483	36419	34261	23468	41952
Independent reflections (R_{int})	19743 (0.0243)	19912 (0.0882)	13859 (0.0275)	12337 (0.0318)	15491 (0.0254)	16038 (0.0667)
R (observed data)	0.0322	0.1061	0.0370	0.0503	0.0697	0.0884
wR (observed data)	0.0764	0.2355	0.0882	0.1045	0.1797	0.1595

CH_2Cl_2 solvent molecules per asymmetric unit. Complex **4a** has 4.5 molecules of CH_2Cl_2 solvates per asymmetric unit. For **5b** the {$SnMe_2Cl$} fragment was triply disordered (occupancies 0.6/0.25/0.15); the Sn atom was refined anisotropically and common isotropic thermal parameters were refined for the remaining disordered fragments. Also, the F atoms of the PF_6 anion are disordered; two octahedra were modeled (occupancies 0.55/0.45) and common isotropic parameters were refined for each model. For **8a**·$2.5CHCl_3$ two phenyl rings showed high mean displacement parameters and no reasonable disorder model could be applied; isotropic thermal parameters were hence refined for the carbon atoms in each ring. The F atoms of the PF_6 anion have high thermal parameters and no reasonable disorder model could be found; individual isotropic thermal parameters were also refined for these F atoms. There are 2.5 $CHCl_3$ molecules per asymmetric unit in four regions and all are disordered. For **9**·$0.5CHCl_3$ the thermal parameter of Br indicates that it may not have full occupancy; the site may also contain Cl. However, there is no evidence in the electron density map. The phenyl carbons of the benzyl groups showed high thermal activity. Since no reasonable disorder model could be found, it is assumed that it may be due to thermal whizzing; isotropic thermal parameters were refined for these C atoms. The F atoms of the PF_6 anion were also disordered; two octahedra were modeled as for **5b**. The lattice contains 0.5 molecule of $CHCl_3$ solvate disordered with occupancies 0.25/0.25. Where present, hydrogen atoms were placed in calculated (d_{C-H} = 0.96 Å) positions.

CCDC reference numbers 160081–160085 and 162463.

See http://www.rsc.org/suppdata/dt/b1/b100789k/ for crystallographic data in CIF or other electronic format.

Acknowledgements

The authors acknowledge the National University of Singapore (NUS) (Grant No. RP 960664/A) for financial support and the technical staff of the Department of Chemistry, NUS for supporting services, in particular, G. K. Tan for assistance with X-ray analysis. S.-W. A. F. is especially grateful to NUS for a research scholarship and for a sponsorship (Grant No. RP 982755) to the University of Waikato as a visiting research scholar. W. H. wishes to thank the University of Waikato and New Zealand Lottery Grants Board for financial support, and Johnson-Matthey Plc for a generous loan of platinum. We are grateful to Professor Brian K. Nicholson (Waikato) for helpful discussions and for donating the tin starting materials.

References

1 M. A. F. Hernandez-Gruel, J. J. Pérez-Torrente, M. A. Ciriano, F. J. Lahoz and L. A. Oro, *Angew. Chem.*, *Int. Ed.*, 1999, **38**, 2769; M. A. Casado, J. J. Pérez-Torrente, M. A. Ciriano, A. J. Edwards, F. J. Lahoz and L. A. Oro, *Organometallics*, 1999, **18**, 5299; A. N. Startsev, *Catal. Rev. Sci. Eng.*, 1995, **37**, 353; T. Murata, Y. Mizobe, H. Gao, Y. Ishii, T. Wakabayashi, F. Nakano, T. Tanase, S. Yano, M. Hidai, I. Echisen, H. Nanikawa and S. Motomura, *J. Am. Chem. Soc.*, 1994, **116**, 3389.

2 (*a*) E. I. Stiefel and K. Matsumoto (Editors), *Transition Metal Sulfur Chemistry: Biological and Industrial Significance*, American Chemical Society, Washington, DC, 1996; (*b*) T. Ikada, S. Kuwata, Y. Mizobe and M. Hidai, *Inorg. Chem.*, 1999, **38**, 64; (*c*) T. Ikada, S. Kuwata, Y. Mizobe and M. Hidai, *Inorg. Chem.*, 1998, **37**, 5793.

3 J. C. Bayón, C. Claver and A. M. Masdeu-Bultó, *Coord. Chem. Rev.*, 1999, **193–195**, 73; M. R. DuBois, *Chem. Rev.*, 1989, **89**, 1.

4 A. V. Firth, E. Witt and D. W. Stephan, *Organometallics*, 1998, **17**, 3716; D. W. Stephan and T. T. Nadasdi, *Coord. Chem. Rev.*, 1996, **147**, 147; D. W. Stephan, *Coord. Chem. Rev.*, 1989, **95**, 41.

5 H. Liu, A. L. Tan, K. F. Mok, T. C. W. Mak, A. S. Batsanov, J. A. K. Howard and T. S. A. Hor, *J. Am. Chem. Soc.*, 1997, **119**, 11006.

6 S.-W. A. Fong and T. S. A. Hor, *J. Chem. Soc.*, *Dalton Trans.*, 1999, 639.

7 M. Capdevila, Y. Carrasco, W. Clegg, R. A. Coxall, P. González-Duarte, A. Lledós and J. A. Ramírez, *J. Chem. Soc.*, *Dalton Trans.*, 1999, 3103; M. Capdevila, Y. Carrasco, W. Clegg, R. A. Coxall,

P. González-Duarte, A. Lledós, J. Sola and G. Ujaque, *Chem. Commun.*, 1998, 597.
8 W. Bos, J. J. Bour, P. P. J. Schlebos, P. Hageman, W. P. Bosman, J. M. Smits, J. A. C. van Wietmarschen and P. T. Beurskens, *Inorg. Chim. Acta*, 1986, **119**, 141.
9 (*a*) M. Zhou, Y. Xu, A.-M. Tan, P.-H. Leung, K. F. Mok, L.-L. Koh and T. S. A. Hor, *Inorg. Chem.*, 1995, **34**, 6425; (*b*) M. Zhou, Y. Xu, L.-L. Koh, A. L. Tan, P.-H. Leung and T. S. A. Hor, *Inorg. Chem.*, 1993, **32**, 1875.
10 C. E. Briant, T. S. A. Hor, N. D. Howells and D. M. P. Mingos, *J. Organomet. Chem.*, 1983, **256**, C15.
11 H. Liu, A. L. Tan, Y. Xu, K. F. Mok and T. S. A. Hor, *Polyhedron*, 1997, **16**, 377.
12 (*a*) H. Liu, A. L. Tan, Y. Xu, K. F. Mok and T. S. A. Hor, *J. Chem. Soc.*, *Dalton Trans.*, 1996, 4023; (*b*) M. Zhou, Y. Xu, C.-F. Lam, P.-H. Leung, L.-L. Koh, K. F. Mok and T. S. A. Hor, *Inorg. Chem.*, 1994, **33**, 1572.
13 (*a*) D. I. Gilmour, M. A. Luke and D. M. P. Mingos, *J. Chem. Soc.*, *Dalton Trans.*, 1987, 335; (*b*) C. E. Briant, T. S. A. Hor, N. D. Howells and D. M. P. Mingos, *J. Chem. Soc.*, *Chem. Commun.*, 1983, 1118; (*c*) C. E. Briant, D. I. Gilmour, M. A. Luke and D. M. P. Mingos, *J. Chem. Soc.*, *Dalton Trans.*, 1985, 851; (*d*) G. W. Bushnell, K. R. Dixon, R. Ono and A. Pidcock, *Can. J. Chem.*, 1984, **62**, 696; (*e*) M. J. Pilkington, A. M. Z. Slawin, D. J. Williams and J. D. Woollins, *J. Chem. Soc.*, *Dalton Trans.*, 1992, 2425.
14 M. Zhou, Y. Xu, C.-F. Lam, L.-L. Koh, K. F. Mok, P.-H. Leung and T. S. A. Hor, *Inorg. Chem.*, 1993, **32**, 4660.
15 V. W.-W. Yam, P. K.-Y. Yeung and K.-K. Cheung, *Angew. Chem., Int. Ed. Engl.*, 1996, **35**, 739.
16 M. Capdevila, W. Clegg, R. A. Coxall, P. González-Duarte, M. Hamidi, A. Lledós and G. Ujaque, *Inorg. Chem. Commun.*, 1998, **1**, 466; G. Li, S. Li, A. L. Tan, W.-H. Yip, T. C. W. Mak and T. S. A. Hor, *J. Chem. Soc.*, *Dalton Trans.*, 1996, 4315.
17 M. Yamashita and J. B. Fenn, *J. Phys. Chem.*, 1984, **88**, 4451; M. Yamashita and J. B. Fenn, *J. Phys. Chem.*, 1984, **88**, 4671.
18 J. B. Fenn, M. Mann, C. K. Meng, S. F. Wong and C. M. Whitehouse, *Science*, 1989, **246**, 64; J. B. Fenn, M. Mann, C. K. Meng, S. F. Wong and C. M. Whitehouse, *Mass Spectrom. Rev.*, 1990, **9**, 37.
19 J. A. Loo and R. R. Ogorzalek-Loo, in *Electrospray Ionisation Mass Spectrometry; Fundamentals*, *Instrumentation and Applications*, ed. R. B. Cole, Wiley-Interscience, New York, 1997, ch. 11; R. D. Smith, J. A. Loo, C. G. Edmonds, C. J. Barinaga and H. R. Udseth, *Anal. Chem.*, 1990, **62**, 882.
20 R. Colton, A. D'Agostino and J. C. Traeger, *Mass Spectrom. Rev.*, 1995, **14**, 79; R. Colton and J. C. Traeger, *Inorg. Chim. Acta*, 1992, **201**, 153; T.-C. Lau, J. Wang, K. W. M. Siu and R. Guevremont, *J. Chem. Soc.*, *Chem. Commun.*, 1994, 1487; C. E. C. A. Hop and R. Bakhtiar, *J. Chem. Educ.*, 1996, **73**, A162; I. I. Stewart and G. Horlick, *Trends Anal. Chem.*, 1996, **15**, 80; C. Moucheron, A. Kirsch-De Mesmaeker, A. Dupont-Gervais, E. Leise and A. van Dorsselaer, *J. Am. Chem. Soc.*, 1996, **118**, 12834; B. H. Lipshutz, K. L. Stevens, B. James, J. G. Pavlovich and J. P. Synder, *J. Am. Chem. Soc.*, 1996, **118**, 6796.
21 W. Henderson, B. K. Nicholson and L. J. McCaffrey, *Polyhedron*, 1998, **17**, 4291; T.-C. Lau, J. Wang, R. Guevremont and K. W. M. Siu, *J. Chem. Soc.*, *Chem. Commun.*, 1995, 877; R. Colton, A. D'Agostino, J. C. Traeger and W. Klaüi, *Inorg. Chim. Acta*, 1995, **233**, 51; G. R. Agnes and G. Horlick, *Appl. Spectrosc.*, 1994, **48**, 655; I. Ahmed, A. M. Bond, R. Colton, M. Jurcevic, J. C. Traeger and J. N. Walter, *J. Organomet. Chem.*, 1993, **447**, 59.
22 T. Løver, W. Henderson, G. A. Bowmaker, J. M. Seakins and R. P. Cooney, *Inorg. Chem.*, 1997, **36**, 3711; T. Løver, G. A. Bowmaker, W. Henderson and R. P. Cooney, *Chem. Commun.*, 1996, 683.
23 L. J. Arnold, *J. Chem. Educ.*, 1992, **69**, 811.
24 (*a*) S. P. Yeo, W. Henderson, T. C. W. Mak and T. S. A. Hor, *J. Organomet. Chem.*, 1999, **575**, 171; (*b*) J. S. L. Yeo, G. Li, W.-H. Yip, W. Henderson, T. C. W. Mak and T. S. A. Hor, *J. Chem. Soc.*, *Dalton Trans.*, 1999, 435; (*c*) C. C. H. Chin, J. S. L. Yeo, Z.-H. Loh, J. J. Vittal, W. Henderson and T. S. A. Hor, *J. Chem. Soc.*, *Dalton Trans.*, 1998, 3777; (*d*) C. Jiang, W. Henderson, T. S. A. Hor, L. J. McCaffrey and Y. K. Yan, *Chem. Commun.*, 1998, 2029.
25 S.-W. A. Fong, J. J. Vittal, W. Henderson, T. S. A. Hor, A. G. Oliver and C. E. F. Rickard, *Chem. Commun.*, 2001, 421.
26 W. Zheng, B.Sc. (Hons) Thesis, National University of Singapore, 1997.
27 Z. Li, X. Xu, S. B. Khoo, K. F. Mok and T. S. A. Hor, *J. Chem. Soc.*, *Dalton Trans.*, 2000, 2901.
28 Z. Li, Z.-H. Loh, K. F. Mok and T. S. A. Hor, *Inorg. Chem.*, 2000, **39**, 5299.
29 W. Henderson, S. J. Faville and B. K. Nicholson, *J. Organomet. Chem.*, 2001, accepted for publication.
30 (*a*) Y. Fuchita, H. Ieda and M. Yasutake, *J. Chem. Soc.*, *Dalton Trans.*, 2000, 271; (*b*) Y. Fuchita, H. Ieda, S. Wada, S. Kameda and M. Mikuriya, *J. Chem. Soc.*, *Dalton Trans.*, 1999, 4431; (*c*) Y. Fuchita, H. Ieda, A. Kayama, J. Kinoshita-Nagaoka, H. Kawano, S. Kameda and M. Mikuriya, *J. Chem. Soc.*, *Dalton Trans.*, 1998, 4095; (*d*) Y. Fuchita, H. Ieda, Y. Tsunemune, J. Kinoshita-Nagaoka and H. Kawano, *J. Chem. Soc.*, *Dalton Trans.*, 1998, 791.
31 J. Chatt and F. A. Hart, *J. Chem. Soc.*, 1960, 2807.
32 J. Chatt and D. M. P. Mingos, *J. Chem. Soc. A*, 1970, 1243.
33 S. P. Gubin, L. A. Polyakova, A. V. Churakov and L. G. Kuz'mina, *Russ. Chem. Bull.*, 1999, **48**, 1757; C. E. Housecroft, D. M. Nixon and A. L. Rheingold, *Polyhedron*, 1999, **18**, 2415; O. Crespo, F. Canales, M. C. Gimeno, P. G. Jones and A. Laguna, *Organometallics*, 1999, **18**, 3142; D. A. Krogstad, V. G. Young and L. H. Pignolet, *Inorg. Chim. Acta*, 1997, **264**, 19.
34 H.-G. Ang, S.-G. Ang and S. Du, *J. Organomet. Chem.*, 1999, **589**, 133; A. D. Hattersley, C. E. Housecroft and A. L. Rheingold, *Inorg. Chim. Acta*, 1999, **289**, 149; D. A. Krogstad, V. G. Young, Jr. and L. H. Pignolet, *Inorg. Chim. Acta*, 1997, **264**, 19; P. M. N. Low, A. L. Tan, T. S. A. Hor, Y.-S. Wen and L.-K. Liu, *Organometallics*, 1996, **15**, 2595; D. M. P. Mingos and M. J. Watson, *Transition Met. Chem.*, 1991, **16**, 285; B. K. Teo and H. Zhang, *Coord. Chem. Rev.*, 1995, **143**, 611.
35 L. H. Pignolet, M. A. Aubart, K. L. Craighead, R. A. T. Gould, D. A. Krogstad and J. S. Wiley, *Coord. Chem. Rev.*, 1995, **143**, 219.
36 L. M. Rendina, J. J. Vittal and R. J. Puddephatt, *Organometallics*, 1996, **15**, 1749.
37 R. Ugo, G. La Monica, S. Cenini, A. Segre and F. Conti, *J. Chem. Soc. A*, 1971, 522.
38 J. S. L. Yeo, J. J. Vittal, W. Henderson and T. S. A. Hor, *J. Chem. Soc.*, *Dalton Trans.*, 2001, 315.
39 A. Bencini, M. D. Vaira, R. Morassi and P. Stoppioni, *Polyhedron*, 1996, **15**, 2079.
40 M. I. Bruce, B. K. Nicholson and O. Bin Shawkataly, *Inorg. Synth.*, 1989, **26**, 325.
41 $AuCl(2\text{-}NC_5H_4PPh_2)$ was synthesized using an analogous method for $AuCl(PPh_3)$ as given in ref. 40.
42 R. Uson, A. Laguna and M. Laguna, *Inorg. Synth.*, 1989, **26**, 86.
43 M. Nonoyama, K. Nakajima and K. Nonoyama, *Polyhedron*, 1997, **16**, 4039.
44 R. W. Fish and M. Rosenblum, *J. Org. Chem.*, 1965, **30**, 1253.
45 V. Baliah and P. Subbarayan, *J. Indian Chem. Soc.*, 1963, **40**, 638.
46 G. B. Deacon and B. O. West, *J. Inorg. Nucl. Chem.*, 1962, **24**, 169.
47 N. A. Bell and L. A. Nixon, *Thermochim. Acta*, 1973, **6**, 275.
48 R. C. Young, *Inorg. Synth.*, 1946, **2**, 25.
49 B. E. Bryant and W. C. Fernelius, *Inorg. Synth.*, 1957, **5**, 113.
50 W. C. Fernelius and J. E. Blanch, *Inorg. Synth.*, 1957, **5**, 130.
51 R. G. Charles, *Inorg. Synth.*, 1963, **7**, 183.
52 D. H. Gerlach and R. A. Schunn, *Inorg. Synth.*, 1974, **15**, 2.
53 B. E. Bryant and W. C. Fernelius, *Inorg. Synth.*, 1957, **5**, 188.
54 R. J. Angelici, *Synthesis and Technique in Inorganic Chemistry*, W. B. Saunders Company, Philadelphia, 1969, p. 153.
55 Modifications from literature procedures, K. Susido, Y. Takeda and Z. Kinugawa, *J. Am. Chem. Soc.*, 1961, **83**, 538.
56 A. J. Gordon and R. A. Ford, *The Chemist's Companion: A Handbook of Practical Data*, *Techniques and References*, Wiley-Interscience, New York, 1972.
57 *SMART & SAINT Software Reference Manuals*, Version 4.0, Siemens Energy & Automation, Inc., Analytical Instrumentation, Madison, WI, 1996.
58 G. M. Sheldrick, SADABS, a Software for Empirical Absorption Correction, University of Göttingen, 1996.
59 G. M. Sheldrick, SHELXTL, Version 5.03, Siemens Energy and Automation Inc., Analytical Instrumentation, Madison, WI, 1996.